NASA TECHNICAL NOTE

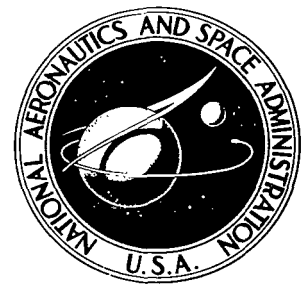

NASA TN D-8476

STATIC AND WIND-ON TESTS OF AN UPPER-SURFACE-BLOWN JET-FLAP NOZZLE ARRANGEMENT FOR USE ON THE QUIET CLEAN SHORT-HAUL EXPERIMENTAL ENGINE (QCSEE)

Arthur E. Phelps III

Langley Directorate,
U.S. Army Air Mobility R&D Laboratory

Langley Research Center
Hampton, Va. 23665

NATIONAL AERONAUTICS AND SPACE ADMINISTRATION • WASHINGTON, D. C. • JUNE 1977

1. Report No. NASA TN D-8476	2. Government Accession No.	3. Recipient's Catalog No.
4. Title and Subtitle STATIC AND WIND-ON TESTS OF AN UPPER-SURFACE-BLOWN JET-FLAP NOZZLE ARRANGEMENT FOR USE ON THE QUIET CLEAN SHORT-HAUL EXPERIMENTAL ENGINE (QCSEE)		5. Report Date June 1977 6. Performing Organization Code
7. Author(s) Arthur E. Phelps III		8. Performing Organization Report No. L-11421
9. Performing Organization Name and Address Langley Directorate, USAAMRDL NASA Langley Research Center Hampton, VA 23665		10. Work Unit No. 505-11-16-11 11. Contract or Grant No.
12. Sponsoring Agency Name and Address National Aeronautics and Space Administration Washington, DC 20546 and U.S. Army Air Mobility R&D Laboratory Moffett Field, CA 94035		13. Type of Report and Period Covered Technical Note 14. Army Project No. 1L161102AH45

15. Supplementary Notes

16. Abstract

An investigation of the internal aerodynamic performance, the static turning characteristics, and the forward-speed characteristics of two 1/12-scale upper-surface-blown jet-flap exhaust-nozzle arrangements designed for use on the Quiet Clean Short-Haul Experimental Engine (QCSEE) has been conducted. The nozzles were equipped with interchangeable area-control side doors in the aft sidewalls of the nozzle so that the effective nozzle area could be varied over a wide range. A simulated wing was used to evaluate installation losses for the nozzles. A smoothly curved flap (Coanda flap) was attached to the trailing edge of the simulated wing to allow an evaluation of the static turning characteristics of the nozzle arrangement. Forward-speed effects on the jet turning characteristics of the QCSEE nozzles were evaluated by mounting a single engine on a semispan wing designed to be representative of a four-engine STOL transport configuration. The low-speed longitudinal aerodynamic performance of the semispan wing equipped with the D-nozzle arrangement was in agreement with the performance obtained with a rectangular nozzle in a previous investigation of a similar wing configuration.

17. Key Words (Suggested by Author(s)) Powered lift STOL QCSEE High-lift nozzles Upper-surface blowing	18. Distribution Statement Unclassified - Unlimited Subject Category 02

19. Security Classif. (of this report) Unclassified	20. Security Classif. (of this page) Unclassified	21. No. of Pages 42	22. Price* $4.00

*For sale by the National Technical Information Service, Springfield, Virginia 22161

STATIC AND WIND-ON TESTS OF AN UPPER-SURFACE-BLOWN JET-FLAP NOZZLE ARRANGEMENT FOR USE ON THE QUIET CLEAN SHORT-HAUL EXPERIMENTAL ENGINE (QCSEE)

Arthur E. Phelps III*
Langley Research Center

SUMMARY

An investigation of the internal aerodynamic performance, the static turning characteristics, and the forward-speed characteristics of two 1/12-scale upper-surface-blown jet-flap exhaust-nozzle arrangements designed for use on the Quiet Clean Short-Haul Experimental Engine (QCSEE) has been conducted. The nozzles were equipped with interchangeable area-control side doors in the aft sidewalls of the nozzle so that the effective nozzle area could be varied over a wide range. A simulated wing was used to evaluate installation losses for the nozzles. A smoothly curved flap (Coanda flap) was attached to the trailing edge of the simulated wing to allow an evaluation of the static turning characteristics of the nozzle arrangement. Forward-speed effects on the jet turning characteristics of the QCSEE nozzles were evaluated by mounting a single engine on a semispan wing designed to be representative of a four-engine STOL transport configuration.

Results of the investigation showed that a D-nozzle incorporating large side doors at the nozzle exit for use in matching the nozzle exit area to the engine cycle requirements had good low-speed jet turning performance. It must be recognized, however, that the final design of a propulsive-lift nozzle must include careful consideration of the cruise drag characteristics and that the nozzle shapes in this report are subject to modifications of the external flow lines to satisfy high-speed cruise requirements. Large increases in jet turning angle were achieved by increasing the jet deflection angle relative to the engine center line up to about 14^{o}, but beyond 14^{o} virtually no improvements in turning angle were observed. Vortex generators had only a small effect on the turning performance of the D-nozzles tested in this investigation, evidently because of the absence of extensive regions of separated flow for which vortex generators are most beneficial. The low-speed longitudinal aerodynamic performance of the semispan wing equipped with the D-nozzle arrangement was in agreement with the performance obtained with a rectangular nozzle in a previous investigation of a similar wing configuration.

INTRODUCTION

The National Aeronautics and Space Administration is presently engaged in the Quiet Clean Short-Haul Experimental Engine (QCSEE) Program to develop

---

*Langley Directorate, U.S. Army Air Mobility R&D Laboratory.

advanced-technology turbofan engines for use on propulsive-lift aircraft. The NASA Lewis Research Center is responsible for overall management of the QCSEE program, and the General Electric Company is the prime contractor for developing and demonstrating the QCSEE propulsion system. The overall objective of the program is to design, build, and test experimental engines for the purpose of consolidating and demonstrating the technology needed for very quiet clean propulsion systems for efficient and environmentally acceptable propulsive-lift aircraft. The program includes the design, fabrication, and testing of two experimental engines, one for the externally blown jet-flap (EBF) concept and one for the upper-surface-blown jet-flap (USB) concept. Because of the close integration of engine and airframe required in development of the USB exhaust nozzle, thrust reverser, and wing-flap arrangement, the NASA Langley Research Center, with its background in USB powered-lift research (for example, see refs. 1 to 3), provided supporting research and technology.

The present investigation, conducted at the Langley Research Center, was aimed at developing a nozzle considered representative of good propulsive-lift technology for the QCSEE USB demonstrator engine. The investigation consisted of two parts conducted on different models: static tests to evaluate the internal aerodynamic performance and jet turning characteristics of three D-shaped nozzle configurations, including the design and analysis of a thrust reverser; and wind-tunnel tests to evaluate the effects of forward speed on the jet turning characteristics of the D-nozzles mounted on a representative propulsive-lift wing design.

The static tests of the present investigation were performed for a range of nozzle pressure ratio on a series of 1/12-scale models of QCSEE engine nozzles mounted on a two-stage turbofan simulator equipped with a bell-mouth inlet. The test program included an evaluation of the effects of changes in nozzle exit area and of the presence of a simulated wing surface on the internal aerodynamic performance of the nozzles. Static turning performance of the nozzles was investigated by attaching a smooth, continuously curved flap (Coanda flap) to the trailing edge of the simulated wing, and the effects of vortex generators and nozzle kickdown angle (the angle at which the thrust vector was caused to impact the wing upper surface) on jet turning characteristics were evaluated. Wind-on tests were performed on a 1/12-scale model of a semispan wing and QCSEE USB engine arrangement considered representative of a propulsive-lift short-haul transport. The model had a full-span leading-edge Krueger flap, a partial-span Coanda flap behind the engine, and a partial-span double-slotted flap between the Coanda flap and the aileron. Tests were performed over a range of angle of attack and thrust coefficient for flap deflections of 0° and 60°.

Results of the static engine-performance tests and thrust-reverser tests are reported in reference 4. Results of the static jet turning tests and the wind-on tests, which are not presented in reference 4, are presented in this report.

SYMBOLS

All data in this report are referred to the aerodynamic stability axis system shown in figure 1. The origin of the axis system for the wind-on force

tests corresponded to an aircraft center-of-gravity position of 25 percent of the wing mean aerodynamic chord.

Measurements and calculations were made in U.S. Customary Units and are presented in both the International System of Units (SI) and U.S. Customary Units. Equivalent dimensions were determined by using the conversion factors given in reference 5.

A_e effective exit area of D-nozzle, obtained by correcting geometric area for boundary-layer losses, cm^2 (in^2)

$A_{e,c}$ effective exit area of D-nozzle in cruise configuration, cm^2 (in^2)

C_D drag coefficient, D/qS

C_L lift coefficient, L/qS

C_m pitching-moment coefficient, $M_Y/qS\bar{c}$

C_μ engine gross-thrust coefficient, T/qS

$\bar{c}$ mean aerodynamic chord, cm (in.)

c_f flap chord, cm (in.)

c_K Krueger flap chord, cm (in.)

c_v vane chord, cm (in.)

c_w local wing chord, cm (in.)

D drag, N (lb)

F_A axial force, N (lb)

F_N normal force, N (lb)

F_{REV} thrust-reverser axial force, N (lb)

$F_{T/O}$ take-off nozzle thrust, N (lb)

L lift, N (lb)

M_Y pitching moment, m-N (ft-lb)

p_o atmospheric pressure, Pa (lb/ft^2)

p_t exhaust duct total pressure, Pa (lb/ft^2)

q free-stream dynamic pressure, $\rho V^2/2$, Pa (lb/ft^2)

S wing area, m^2 (ft^2)

T gross static thrust, N (lb)

V velocity, m/sec (ft/sec)

α angle of attack, deg

γ flight-path angle, deg

θ_j nozzle kickdown angle, angle relative to engine center line at which thrust vector impacts wing upper surface, deg

δ_f total flap deflection, deg

δ_j static jet deflection angle, positive downward, deg

η_j static thrust-recovery efficiency, $\sqrt{F_N^2 + F_A^2}/T$

ρ air density, kg/m^3 (slugs/ft^3)

Abbreviations:

B.L. baseline

MOD. modified

NPR nozzle pressure ratio, p_t/p_o

QCSEE Quiet Clean Short-Haul Experimental Engine

Sta. wing station (see fig. 7(a))

USB upper-surface blown

V.G. vortex generators

BACKGROUND OF MODEL AND APPARATUS DEVELOPMENT

The QCSEE USB engine is an advanced-technology, high-bypass-ratio (B.P.R. of 10) turbofan engine designed to exhaust both the fan and the core flows into a single exhaust duct and nozzle. Figure 2(a) shows a sketch of the QCSEE USB nacelle design in the cruise configuration. The D-shaped exhaust nozzle was chosen to minimize cruise drag penalties which may be expected from the presence of the nacelle on the wing upper surface (see ref. 6). The QCSEE demonstrator engine requires approximately a 20-percent increase in effective exit area of the nozzle as the engine total pressure ratio is reduced from the cruise value of 1.85 to the take-off value of 1.29, as shown in figure 2(b).

Although there are a number of reasons for this large variation in exit area, one of the main reasons is to maintain a constant inlet weight flow (or very nearly so) over the operational range of engine pressure ratio. The reason for this is that the QCSEE inlet is designed to have a high subsonic throat Mach

number for acoustic suppression of forward-radiated fan noise, whereas the fan is designed to produce high take-off thrust at a low pressure ratio (1.29) in order to reduce exhaust noise. Thus, a large exit is required for take-off in order to maintain high inlet flow and, hence, high subsonic throat Mach number at a low pressure ratio. At cruise airspeeds, however, it is desirable to operate at the highest possible pressure ratio compatible with the surge characteristics of the fan in order to optimize cruise efficiency; the high pressure ratio requires a smaller exit area. Although this particular requirement is applicable to any turbofan engine, it is somewhat more severe for the QCSEE engine with its very high bypass ratio.

The method selected for achieving the large area variation is the use of large doors mounted in the aft sidewalls of the nozzle and hinged along their upper edge so that they open outward as shown in figure 2(c). There are, of course, many different ways of incorporating some variable geometry features into the nozzle, but large side doors serve the dual purpose of increasing the exit area of the nozzle while at the same time spreading the exhaust jet spanwise along the wing and directing the flow downward toward the wing upper surface to help thin the jet. Figure 2(d) shows the results of some flow visualization tests of a small model with the doors closed and open and illustrates the significant spanwise spreading of the jet with the doors open.

The objective of the static turning tests was to achieve, at an approach nozzle pressure ratio of 1.19, a high jet turning angle (57° to 60°) at high thrust-recovery efficiency for a typical approach flap setting of 60° using a D-shaped nozzle suitable for cruise applications. During this test program, three different D-nozzle configurations were tested and the essential differences are shown in figure 3. A "baseline nozzle," designed using the results of previous work reported in references 3 and 6, served as a starting point for the nozzle development. The other two nozzles were modified to increase nozzle kickdown angle after a series of initial screening tests with the baseline nozzle. The first modification involved a slight flattening of the cross-section contours of the nozzle roof upstream of the exit, an increase in the longitudinal roof angle upstream of the exit, and also an increase in the angle of the nozzle floor with respect to the wing. The second modification also used increased floor angle at the nozzle exit, but the original cross-section roof contours and exit shape were retained, and the roof angle at the exit was increased, thereby increasing the external boattail angle. Both the exit shape and the geometric exit area were held constant for all three nozzles.

Although an analysis of the internal aerodynamic performance and propulsive efficiency of the D-nozzles is reported in reference 4 as explained previously, a summary of the performance of the side doors in increasing the effective exit area of each of the nozzles is repeated in figure 4 for convenience. The data show that modified nozzle number 2 had only a 17-percent increase in effective exit area, whereas modified nozzle number 1 had an increase in effective exit area of 19.5 percent. For this reason no further tests were conducted on modified nozzle number 2. All tests discussed in the present report were conducted on the baseline nozzle and modified nozzle number 1, hereafter referred to as the modified nozzle. One important result reported in reference 4 is that both the baseline nozzle and the modified nozzle had good propulsive efficiency, so

that there was not a significant engine penalty for the relatively high kickdown angle of the modified nozzle.

An additional requirement of the QCSEE USB nozzle is that it contain a means for providing reverse thrust. The thrust reverser is required to provide a maximum reverse thrust component equal to 35 percent of the maximum available take-off thrust at a nozzle pressure ratio of 1.29, while providing for an inlet weight flow of not less than 80 percent of the take-off weight flow. The reason for the minimum weight flow requirement for the full-scale engine is to insure adequate surge margin for the fan when the thrust reverser is deployed.

Figure 5(a) shows a sketch of the single-target thrust-reverser concept used on the QCSEE USB nozzle. In its original form, the thrust reverser had a shorter deflector lip and did not incorporate the "side skirts" shown on the figure. Initial testing showed that a very large amount of the engine flow was not being turned by the blocker door because of the comparatively small capture area, and the reverse-thrust efficiency was very poor as shown in figure 5(b). A series of development tests led to incorporation of the articulated side skirts shown on figure 5(a), along with a longer deflector lip. The result of these modifications on reverse-thrust efficiency is presented in figure 5(b), which shows that the reverser met the reverse-thrust requirements $\left(\frac{F_{REV}}{F_{T/O}} = 0.35\right)$ at a total pressure ratio of 1.29. The detailed thrust-reverser analysis is presented in reference 4.

MODELS

Two types of models were used in the test program: static test nozzles used in the nozzle development tests, and a wind-tunnel model used in wind-on tests. These two model types are discussed separately in this section.

Static Models

The engine simulator used in the static investigation was a 13.97-cm (5.5-in.) diameter, two-stage, turbofan simulator composed of two commercially available single-stage simulators in a tandem arrangement shown in figure 6(a). This arrangement was used because the maximum pressure ratio of 1.2 available from a single simulator would not allow testing at the QCSEE take-off pressure ratio of 1.29. The maximum pressure ratio available with the tandem-fan simulator was about 1.3. There was no mechanical connection between the two simulators. The fans were mounted on a manifold which supplied drive air to both turbines and which incorporated two throttling valves for individual adjustment of the drive-air supply to each fan; compressed air was supplied to the manifold through the engine mounting strut. A bell-mouth inlet was attached to the front face of the simulator, and the aft end of the simulator was equipped with a flange on which the test nozzles could be mounted.

Three nozzle configurations were tested as previously described. Each nozzle was fabricated from a fiberglass-epoxy laminate laid up over a properly con-

toured male pattern; thus, only the internal flow lines were accurately defined. Eight total pressure rakes were mounted around the circumference of each nozzle for measuring the duct total pressure. Provision was made at the aft sidewalls of each nozzle for mounting interchangeable side doors.

Each nozzle was provided with a mounting arrangement for attaching a simulated wing upper surface to the underside of the nozzle and could be tested with the simulated wing attached or removed. Static turning data were measured by attaching a curved flap, or Coanda flap, to the trailing edge of the simulated wing. (See table I for coordinates of Coanda flap on the static model.) In addition, some static turning data were obtained with vortex generators mounted just ahead of the knee of the flap. Two shapes of vortex generators were tested: rectangular and delta. The curvature of the Coanda flap was designed to correspond to the wind-tunnel wing described subsequently in this section. Details of the simulated wing, Coanda flap, and vortex generators are shown in figures 6(b) and 6(c).

Wind-Tunnel Model

Wind-tunnel tests were conducted on the single-engine semispan model shown in figure 7(a). The full-scale QCSEE engine is envisioned as being used on a four-engine USB powered-lift aircraft having an installed thrust-weight ratio of 0.6. The semispan wing used in the wind-tunnel tests was derived by scaling a wing which had been designed to meet these full-scale considerations. Although a semispan model of a four-engine aircraft would properly have two engines, only one engine was mounted on the model at a position midway between the positions normally occupied by two engines. This was done because the purpose of the wind-tunnel tests was only to evaluate the effect of forward speed on the turning characteristics of the D-nozzle in the low-speed configuration, and previous experience had shown that interference effects between two adjacent jets were not of a type to reduce the turning performance of either jet.

Power for the model was provided by a single-stage turbofan simulator shown in figure 7(b). A single-stage simulator was used on the wind-tunnel model for two reasons: first, the tandem-fan simulator used on the static test model was too long to allow the external dimensions of the full-scale nacelle to be modeled; and second, the jet turning tests, for which the wind-tunnel test program was conducted, were performed for the landing configuration since that is the most severe case for jet turning. The QCSEE design nozzle pressure ratio for the landing condition is 1.19, and this value was within the capabilities of the single-stage simulator. Both the baseline nozzle and the modified nozzle were tested with a cruise door configuration (Door angle = 0°) for reference purposes and a low-speed door configuration (Door angle = 25°). Details of the engine installation are shown in figure 7(b).

The wing leading edge was equipped with a two-segment Krueger flap, one segment extending from the wing root to the inboard side of the nacelle, and the second segment extending from the outboard side of the nacelle to the wing tip. Wing trailing-edge high-lift devices consisted of a smoothly curved, constant-chord Coanda flap behind the engine extending from the wing root to the midsemispan wing station, and a partial-span double-slotted flap between the Coanda

flap and the aileron. Provision was made for installation of a chord extension along the trailing edge of the Coanda flap and for installation of vortex generators just forward of the knee of the flap, as was the case for the static model. Details of positions and deflections of the leading-edge and trailing-edge high-lift devices are presented in figure 7(c). Coordinates are given for the Coanda flap in table II, for the wing airfoil sections in table III, for the two elements of the double-slotted flap in table IV, and for the leading-edge Krueger flap in table V.

TESTS AND PROCEDURES

The test program was conducted in two phases: static tests followed by wind-on tests. The static tests included an evaluation of the internal aerodynamic performance for both the high-speed and the low-speed configurations and an evaluation of the jet turning performance of the various configurations under study. The wind-on tests investigated the effects of forward speed on the propulsive-lift characteristics of the nozzles and wing assembly.

Static Tests

In preparation for the tandem-fan nozzle development tests, a series of round-nozzle calibration tests were conducted on the tandem-fan simulator. The exit areas of the calibration nozzles were chosen to include the complete range of effective exit area which occurs as the side doors in the D-nozzles are opened from their cruise position to the final landing position. Tests were made on each calibration nozzle by varying engine rotational speed (rpm) and measuring thrust, drive-air weight flow, inlet static pressures, and exhaust duct total pressures at each speed. In addition, local temperature and barometric pressure were recorded at each test speed. All calibration tests and D-nozzle static tests were made with the bell-mouth inlet shown in figure 6(a).

After the simulator calibration tests, the D-nozzles were each tested according to the following general outline:

1. Nozzle-alone tests (no simulated wing). Side-door angles = 0°, 20°, 25°, and 30°.[1]

2. Nozzle with simulated wing. Side-door angles = 0°, 20°, 25°, and 30°.[1]

3. Static turning tests (nozzle with simulated wing and Coanda flap). Side-door angle = 25°:

   a. Without vortex generators

   b. With vortex generators

[1]The effect of door angle on internal aerodynamic performance is reported in reference 4.

A few static turning tests were also performed with the wind-tunnel model, in which the effects of kickdown angle over a range from 10° to 16° were investigated by tilting the entire engine assembly on the wing.

The value of gross thrust used in the D-nozzle static performance evaluation was computed to be the resultant of the measured normal and axial forces $\left(T = \sqrt{F_N^2 + F_A^2}\right)$ with the simulated wing in place but with the Coanda flap removed. For the wind-tunnel model, the engine calibration was performed with the engine mounted on the wing and with the trailing-edge flaps in the retracted position.

The D-nozzle development tests were performed in the static test area of the Langley full-scale tunnel. Force measurements were made using a three-component strain-gage balance, and bell-mouth inlet static pressures and exhaust duct total pressures were measured by means of pressure transducers. A commercially available drive-air flowmeter was mounted just upstream of the balance and was used to measure drive-air mass flow to the engine simulator. For safety purposes, bearing temperatures and rotational speed of each fan were monitored during all static tests.

Wind-On Tests

Wind-on tests were run for the cruise flap setting ($\delta_f = 0^{\circ}$) and the landing flap setting ($\delta_f = 60^{\circ}$) over an angle-of-attack range from about -4° to 36°. The range of thrust coefficient was from 0 to 2.0 for the cruise configuration and from 0 to 4.0 for the landing configuration. The power-on tests were run by setting the engine speed to provide the desired level of static thrust (determined in the static engine calibration) and by holding this speed constant throughout the angle-of-attack range. At the tunnel speeds used in investigations of this type, experience with other models (ref. 1) has shown that the effect of forward velocity on the gross thrust of the engine simulators is very small, and it is gross thrust that is used in defining C_{μ}.

The C_{μ} range was obtained by varying both the engine thrust and the tunnel speed. The free-stream dynamic pressure for the power-off tests was 230 Pa (4.81 lb/ft^2) for an airspeed of 19.4 m/sec (63.57 ft/sec) and a Reynolds number of 6.10×10^5 based on the wing mean aerodynamic chord. For the power-on tests the free-stream dynamic pressure varied from 80.44 Pa (1.68 lb/ft^2) to 230 Pa (4.80 lb/ft^2) for an airspeed range from 11.5 m/sec (37.7 ft/sec) to 19.4 m/sec (63.67 ft/sec) and a Reynolds number range from 3.62×10^5 to 6.10×10^5.

Tests were performed in the 3.66-m (12-ft) octagonal test section of a low-speed wind tunnel at the Langley Research Center, and wall corrections determined empirically from reference 7 were applied to the data. All tests were made with the model mounted vertically in the tunnel on a five-component (no side-force beam) strain-gage balance. Figure 8 shows the model mounted in the tunnel for force testing.

RESULTS AND DISCUSSION

Static Tests

Results of tests to determine the static turning characteristics of the baseline and modified D-nozzles in the low-speed configuration are presented in figure 9. The data show that the baseline nozzle was deficient in meeting the static turning goals previously discussed. Flow visualization studies using both tufts and oil-flow techniques showed reasonably well-attached flow extending to the trailing edge of the flap with some small regions of separated flow, but there was evidence of substantial jet thickening and side vortex rollup as the jet turned downward over the surface of the Coanda flap. Vortex generators were attached to the Coanda flap as shown in figure 6(c) in an attempt to spread the jet further spanwise and to break up the large vortex at the sides of the jet sheet. The data of figure 9 show that the vortex generators had only a small effect on the turning characteristics of the baseline nozzle and an insignificant effect on the turning characteristics of the modified nozzle. This result was evidently due to the fact that there were no large regions of separated flow for which vortex generators would be expected to be most beneficial. It should be noted that the vortex generators used in these tests were not optimized but were tested only to give an indication of the gross effects that might be expected from their use. The comparatively low jet turning angle obtained with the baseline nozzle appeared to be primarily a result of insufficient spanwise spreading of the jet before it began to turn downward over the Coanda flap. Nozzle-alone tests of the baseline nozzle showed that the nozzle kickdown angle was about 9° (ref. 4); so the modified nozzle was designed to have increased kickdown angle as previously described.

Tests to evaluate the effectiveness of increased nozzle kickdown angle on static turning were conducted on the wind-tunnel wing-flap assembly with the modified nozzle, and the results are presented in figure 10 for kickdown angles of 10°, 14°, and 16°. The data show a large increase in turning angle as nozzle kickdown angle was increased from 10° to 14°, but practically no effect as the kickdown angle was further increased to 16°. Note that the turning angle obtained with the nozzle set at 10° is about 49°, which is the same value obtained with the baseline nozzle at NPR = 1.2 (fig. 9). Tufts attached to the surface of the wing showed an increase in the spanwise spreading of the exhaust as the nozzle kickdown angle was increased from 10° to 14°, but no significant increase in spreading when the kickdown angle was increased from 14° to 16°. Increasing the flap chord by adding an extension to the trailing edge of the Coanda flap produced a small increase in jet turning angle, with no significant loss in turning efficiency. The data of figure 9(b) show that thrust-recovery efficiencies were generally fairly high, about 84 to 90 percent, but both vortex generators and kickdown angle caused a reduction in efficiency.

Wind-On Tests

The longitudinal aerodynamic characteristics of the wing with the baseline nozzle are presented in figures 11(a) and 11(b) for the cruise and landing configurations, respectively. The data show the characteristic increase in maximum lift coefficient, stall angle of attack, and negative pitching-moment coefficient

with increasing thrust coefficient; a maximum lift coefficient of about 8.5 was achieved for the model in the landing configuration. The large negative pitching-moment coefficients accompanying the high lift coefficients are characteristic of powered-lift configurations but are somewhat more severe than those obtained from swept wing models of previous investigations (for example, ref. 1).

Tufts attached to the upper surface of the wing and flap showed that the jet spreading under forward flight conditions was nearly identical with that observed in the static case. Thus, the relatively low resultant turning angle for the baseline nozzle appears to be due to the thickness of the jet rather than to surface separation, since both the wind-on and wind-off tests showed well-attached surface flow extending to the trailing edge of the Coanda flap.

The effect of the relatively low turning angle on the aerodynamic characteristics of the baseline nozzle is shown in the drag polar of figure 11(b). At the present time there are no certified requirements for approach performance of powered-lift aircraft; for the purpose of comparative analysis, an approach lift coefficient of 4.0, a 6° glide slope, and 15° stall margin are considered representative criteria. The data show that the baseline nozzle produced fairly high lift coefficients, but there was too little drag to provide acceptable descent capability, and the stall margin was only about 9°.

Data for the baseline nozzle with vortex generators, presented in figure 12, indicate a significant improvement in lift performance when compared with the baseline nozzle for the same thrust coefficient, even though the static turning angle was only moderately increased (approximately 2°). In addition to the increased lift obtained through the use of vortex generators, there was also a significant increase in drag, evidently as a result of the lower thrust-recovery efficiency, and the drag polars of figure 12 indicate good descent capability at an approach lift coefficient of 4.0, with the stall margin increased to about 12°.

Although these data indicate that the baseline nozzle could produce acceptable low-speed aerodynamic performance when used in conjunction with vortex generators, it was desired to use a nozzle which did not require a secondary or external means for achieving the required low-speed turning performance. The remainder of the wind-on test program was therefore conducted with the modified nozzle.

Results of tests to determine the effect of kickdown angle on the aerodynamic performance of the modified nozzle in the landing configuration are presented in figures 13(a), 13(b), and 13(c) for nozzle kickdown angles of 10°, 14°, and 16°, respectively. The data show a significant increase in both lift and drag coefficients as kickdown angle was increased from 10° to 14°, but only a very small change as kickdown angle was further increased to 16°. Tuft studies with the wind on showed attached flow for all the cases tested, but there was significantly more spanwise spreading for the 14° nozzle setting than for the 10° nozzle setting, as expected on the basis of results of static tests. Virtually no difference in wind-on flow spreading was observed for the 14° and 16° nozzles; for this reason, the test program was conducted with the modified nozzle set at its design kickdown angle of 14°. Comparison of the drag polars of figure 13(b) for the modified nozzle with those of figure 12 for the baseline

nozzle with vortex generators indicates similar descent capability for the two configurations, although the modified nozzle did produce slightly higher maximum lift coefficients than the baseline configuration.

For an approach lift coefficient of 4.0, the model with the modified nozzle would be required to fly at an angle of attack of about 8° and a thrust coefficient of about 0.9 (see fig. 13(b)). In order to reduce the approach angle of attack, an effort was made to increase lift with a flap chord extension which produced a 10-percent increase in flap chord (measured along the engine center line), and results of tests of this configuration are shown in figure 14. The data indicate a modest increase in both lift and drag of the configuration with the flap chord extension, as well as a slight (approximately 2°) increase in stall angle of attack. Static turning data for this configuration indicate that the use of the flap chord extension resulted in virtually no change in the measured static turning angle.

Figure 15 presents a comparison of the drag polars of the configuration of figure 14 (modified nozzle and flap chord extension) with those of the configuration of figure 11(b) (baseline nozzle). The data show that both configurations could fly the selected approach condition (C_L = 4.0 and γ = -6°) at a thrust coefficient of about 0.9, but the modified configuration had a significantly improved stall margin. From the lift data of figures 11(b) and 14 for these two configurations, it can be seen that the baseline configuration had about 9° stall margin at C_L = 4.0 and C_μ = 0.9, whereas the modified configuration had a 15° stall margin at these conditions. In addition, use of the modified nozzle and flap chord extension reduced the approach angle of attack from 12.5° for the baseline configuration to 6° for the modified configuration.

In order to assess the low-speed performance of the D-nozzle compared with rectangular nozzles of earlier investigations, figure 16 presents a comparison of the drag polar of the modified configuration of the present investigation with the drag polar of the twin-engine, straight-wing configuration of reference 8, which had a rectangular nozzle. The data for the model of reference 8 have been plotted for the configuration which produced the same jet turning angle as the modified configuration of the present study, and show generally comparable descent capabilities for the two configurations.

SUMMARY OF RESULTS

Static and wind-on tests of D-nozzles designed for the Quiet Clean Short-Haul Experimental Engine (QCSEE) for the upper-surface-blown jet-flap concept have been conducted. The results may be summarized as follows:

1. A D-nozzle incorporating large side doors at the nozzle exit for use in matching the nozzle exit area to the engine cycle requirements has been shown to have good low-speed jet turning performance. It must be recognized, however, that the final design of a propulsive-lift nozzle must include careful consideration of the cruise drag characteristics, and that the nozzle shapes in this report are subject to modification of the external flow lines to satisfy high-speed cruise requirements.

2. The original nozzle design was deficient in meeting the static turning goal (jet turning angle of 57° to 60°), but large increases in jet turning angle were achieved by increasing nozzle kickdown angle up to about 14°. Increasing kickdown angle from 14° to 16° resulted in virtually no improvements in turning angle.

3. Vortex generators had only a small effect on the turning performance of the D-nozzles tested in this investigation, probably because of the absence of extensive regions of separated flow for which vortex generators are most beneficial.

4. The low-speed longitudinal aerodynamic performance of a semispan model of a four-engine USB configuration equipped with a modified QCSEE D-nozzle was generally in agreement with the performance obtained with rectangular nozzles in a previous investigation of a similar configuration.

Langley Research Center
National Aeronautics and Space Administration
Hampton, VA 23665
April 20, 1977

REFERENCES

1. Phelps, Arthur E., III; and Smith, Charles C., Jr.: Wind-Tunnel Investigation of an Upper Surface Blown Jet-Flap Powered-Lift Configuration. NASA TN D-7399, 1973.

2. Parlett, Lysle P.; Greer, H. Douglas; Henderson, Robert L.; and Carter, C. Robert: Wind-Tunnel Investigation of an External-Flow Jet-Flap Transport Configuration Having Full-Span Triple-Slotted Flaps. NASA TN D-6391, 1971.

3. STOL Technology. NASA SP-320, 1972.

4. Ammer, R. C.; and Kutney, J. T.: Analysis and Documentation of QCSEE (Quiet Clean Short-Haul Experimental Engine) Over-the-Wing Exhaust System Development. NASA CR-2792, 1977.

5. Mechtly, E. A.: The International System of Units - Physical Constants and Conversion Factors (Second Revision). NASA SP-7012, 1973.

6. Skavdahl, Howard; Wang, Timothy; and Hirt, William J.: Nozzle Development for the Upper Surface-Blown Jet Flap on the YC-14 Airplane. [Preprint] 740469, Soc. Automot. Eng., Apr.-May 1974.

7. Phelps, Arthur E.; Letko, William; and Henderson, Robert L.: Low-Speed Wind-Tunnel Investigation of a Semispan STOL Jet Transport Wing-Body With an Upper-Surface Blown Jet Flap. NASA TN D-7183, 1973.

8. Smith, Charles C., Jr.; Phelps, Arthur E., III; and Copeland, W. Latham: Wind-Tunnel Investigation of a Large-Scale Semispan Model With an Unswept Wing and an Upper-Surface Blown Jet Flap. NASA TN D-7526, 1974.

TABLE I.- COORDINATES OF COANDA FLAP USED ON STATIC MODEL

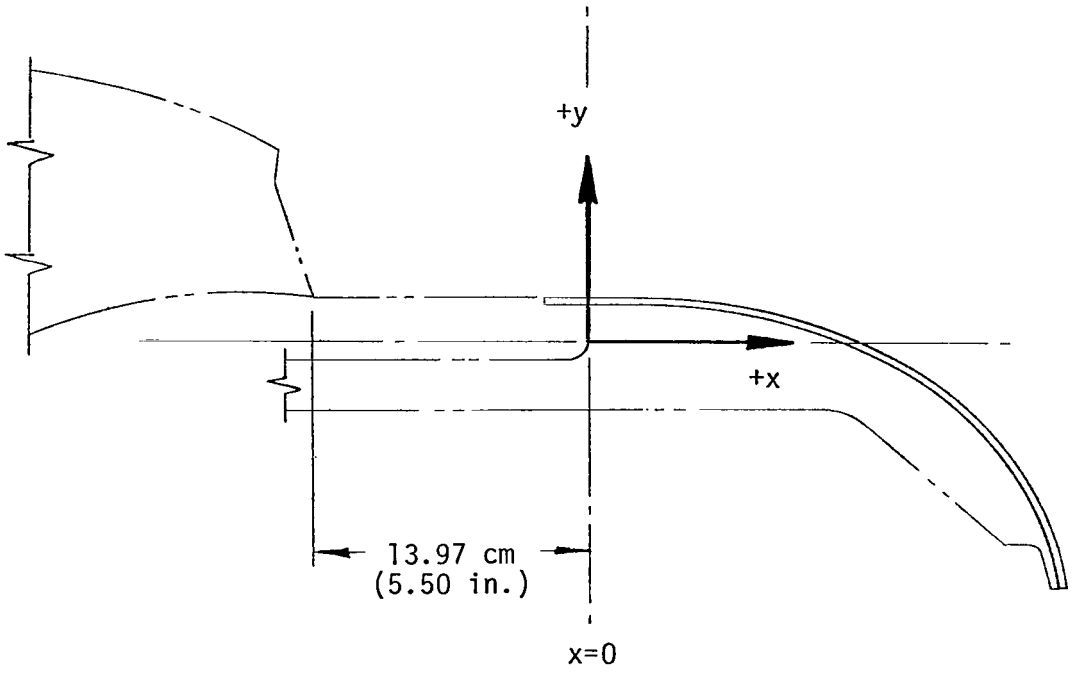

x		y	
cm	in.	cm	in.
0	0	3.38	1.33
2.54	1.00	3.38	1.33
7.62	3.00	2.95	1.16
12.70	5.00	1.96	.77
15.24	6.00	1.30	.51
17.78	7.00	-.33	-.13
20.32	8.00	-2.34	-.92
21.59	8.50	-3.71	-1.46
22.86	9.00	-5.41	-2.13
24.13	9.50	-7.59	-2.99
24.77	9.75	-9.04	-3.56
25.40	10.00	-11.20	-4.41
26.04	10.25	-13.67	-5.38

TABLE II.- COORDINATES OF COANDA FLAP USED ON WIND-TUNNEL MODEL

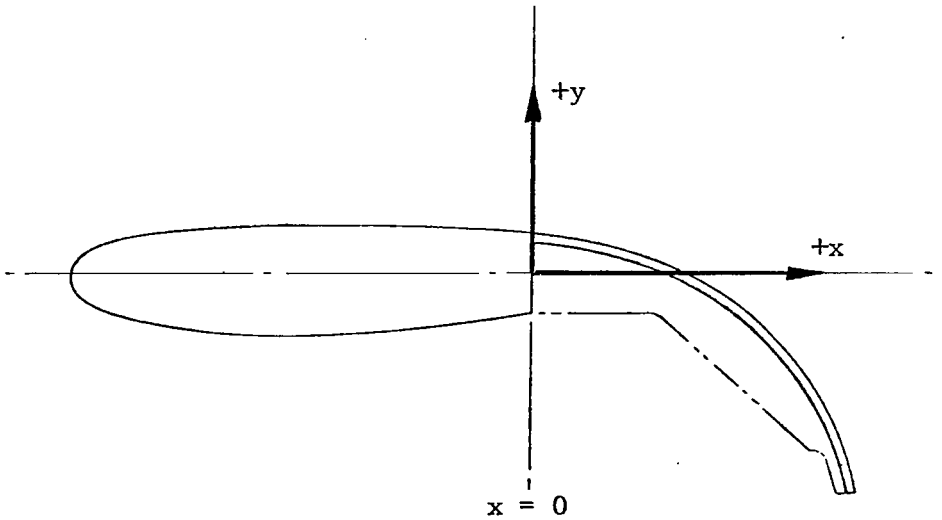

x		y	
cm	in.	cm	in.
0	0	3.95	1.55
5.08	2.00	3.43	1.35
10.16	4.00	2.60	1.02
15.24	6.00	1.07	.42
17.78	7.00	-.28	-.11
20.32	8.00	-2.31	-.91
21.59	8.50	-3.64	-1.43
22.86	9.00	-5.31	-2.09
24.13	9.50	-7.54	-2.97
25.40	10.00	-11.18	-4.40
26.04	10.25	-13.56	-5.34

TABLE III.- COORDINATES OF WING AIRFOIL SECTIONS USED ON WIND-TUNNEL MODEL

[Dimensions are given in percent local wing chord]

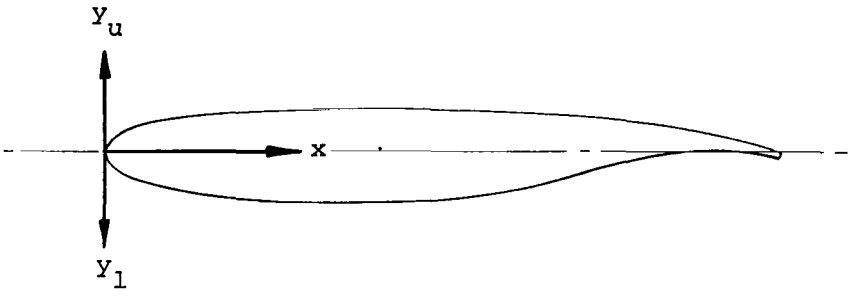

x	Sta. 0		Sta. 35.00		Sta. 70.00	
	y_u	y_l	y_u	y_l	y_u	y_l
0	0	0	0	0	0	0
1.25	2.96	-2.89	2.92	-3.12	2.18	-2.17
2.50	3.93	-3.74	3.97	-4.14	2.76	-2.80
5.00	5.14	-4.78	5.42	-5.34	3.48	-3.58
7.50	5.97	-5.35	5.91	-6.06	3.95	-4.09
10.00	6.57	-5.80	6.48	-6.58	4.29	-4.46
15.00	7.33	-6.38	7.33	-7.30	4.77	-4.94
20.00	7.80	-6.79	7.92	-7.77	5.08	-5.23
25.00	8.09	-7.00	8.31	-8.04	5.27	-5.41
30.00	8.23	-7.14	8.61	-8.18	5.40	-5.49
35.00	8.25	-7.24	8.80	-8.16	5.47	-5.49
40.00	8.25	-7.28	8.92	-8.05	5.50	-5.25
50.00	8.09	-7.16	8.85	-7.37	5.45	-4.98
60.00	7.53	-6.43	8.34	-5.87	5.21	-3.90
70.00	6.56	-4.57	7.36	-1.56	4.74	-1.51
80.00	5.12	-2.05	5.61	-.13	3.96	.53
90.00	3.00	-.25	3.14	-.22	2.56	1.40
95.00	1.64	-.14	1.62	-.45	1.45	1.07
100.00	0	-.62	0	-.77	-.08	-.14

TABLE IV.- COORDINATES OF DOUBLE-SLOTTED FLAP USED ON WIND-TUNNEL MODEL

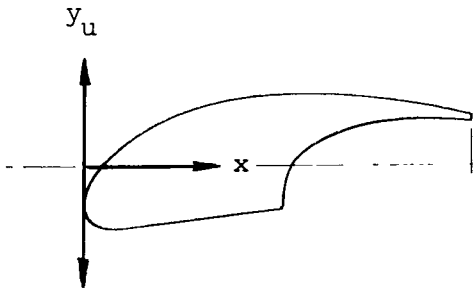

VANE

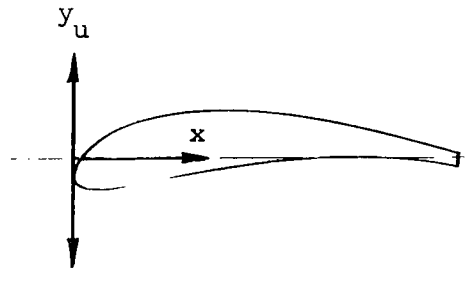

FLAP

x, percent c_v or c_f	Coordinates for vane, percent c_v				Coordinates for flap, percent c_f			
	Sta. 35.00		Sta. 52.50		Sta. 35.00		Sta. 52.50	
	y_u	y_l	y_u	y_l	y_u	y_l	y_u	y_l
0	-12.50	-12.50	-8.00	-8.00	-4.00	-4.00	-2.50	-2.50
1.25	-6.52	-16.50	-3.50	-12.60	0	-7.38	1.50	-5.05
2.50	-4.00	-18.09	-1.48	-14.00	1.92	-8.42	3.25	-5.85
5.00	-.30	-19.49	1.65	-15.50	4.79	-8.70	5.32	-6.48
7.50	3.55	-20.20	3.90	-16.27	6.93	-8.45	6.60	-6.68
10.00	4.82	-20.48	5.75	-16.65	8.68	-7.87	7.56	-6.56
15.00	8.50	-20.13	8.90	-16.65	11.01	-6.70	9.08	-5.76
20.00	11.52	-19.19	11.25	-16.10	12.64	-5.64	10.20	-4.84
25.00	14.10	-17.98	13.11	-15.20	13.78	-4.67	11.06	-3.98
30.00	16.28	-16.51	14.65	-14.02	14.52	-3.75	11.65	-2.15
40.00	19.40	-13.82	16.92	-11.70	15.06	-2.15	12.11	-1.72
50.00	21.05	-11.50	18.10	-9.60/-2.00	14.25	-1.02	11.90	-.69
52.00	21.24	1.10	18.25	2.90	-----	-----	-----	-----
54.00	21.42	4.10	18.33	4.80	-----	-----	-----	-----
60.00	21.84	9.98	18.40	8.30	12.32	-.43	10.95	0
70.00	21.82	13.50	18.23	11.32	9.75	-.46	9.30	.15
80.00	21.13	15.85	17.70	12.92	6.68	-1.00	7.17	0
90.00	19.91	16.71	16.63	13.50	3.25	-1.79	4.75	-.60
100.00	18.00	16.55	15.28	13.50	-.43	-2.70	2.11	-1.45
	$c_v = 0.236c_w$		$c_v = 0.233c_w$		$c_f = 0.264c_w$		$c_f = 0.262c_w$	

TABLE V.- COORDINATES OF KRUEGER FLAP USED ON WIND-TUNNEL MODEL

[Dimensions given in percent Krueger flap chord]

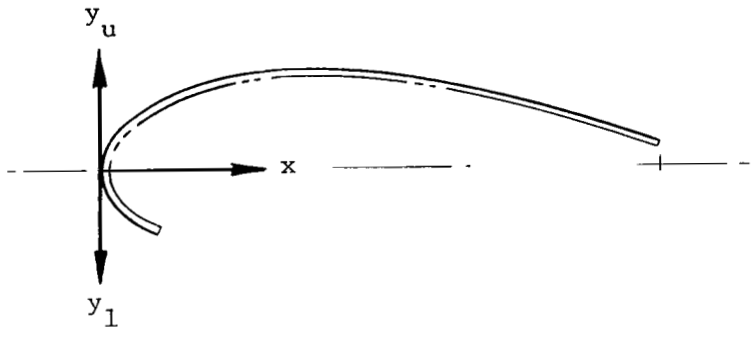

x	Sta. 0		Sta. 35.00		Sta. 70.00	
	y_u	y_l	y_u	y_l	y_u	y_l
0	0	0	0	0	0	0
1.25	5.00	-5.00	5.00	-5.00	5.00	-5.00
2.50	6.95	-6.95	6.95	-6.95	6.95	-6.95
5.00	10.00	-10.00	10.00	-10.00	10.00	-10.00
7.50	12.05	-12.05	12.00	-12.05	12.00	-12.05
10.00	13.55	-13.55	13.55	-13.55	13.55	-13.55
15.00	15.60	-15.60	15.60	-15.60	15.95	-15.95
20.00	16.95	------	16.95	------	17.50	------
30.00	17.90	------	17.90	------	19.20	------
40.00	17.50	------	17.50	------	19.35	------
50.00	16.20	------	16.20	------	18.62	------
60.00	14.20	------	14.20	------	17.25	------
70.00	11.60	------	11.60	------	15.30	------
80.00	8.55	------	8.55	------	12.80	------
90.00	5.25	------	5.25	------	9.90	------
100.00	1.70	------	1.70	------	6.70	------
	$c_K = 0.17c_w$		$c_K = 0.22c_w$		$c_K = 0.175c_w$	

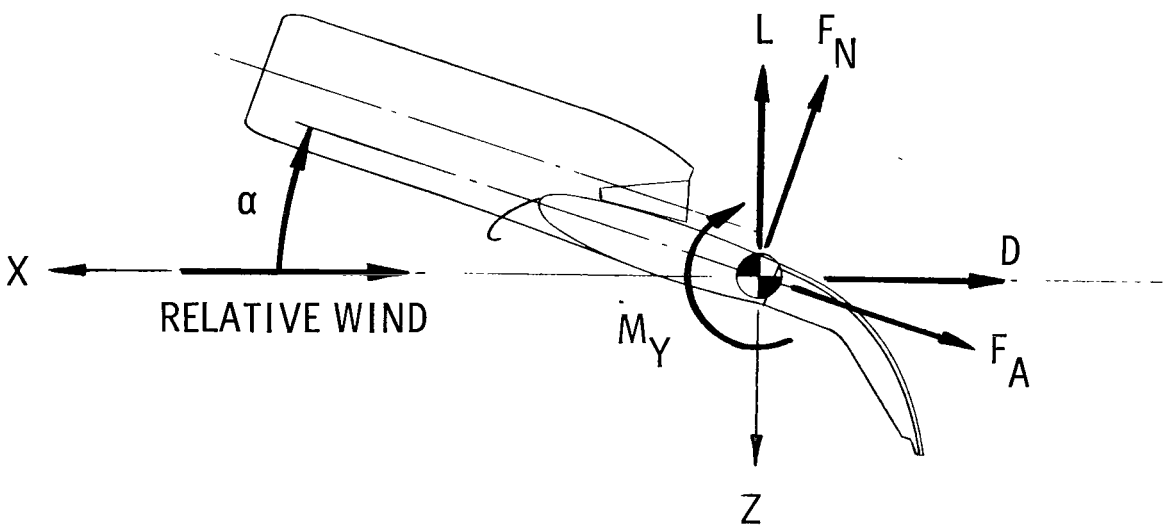

Figure 1.- Coordinate system used in presentation of data. Arrows denote positive directions of forces, moments, and angular displacements.

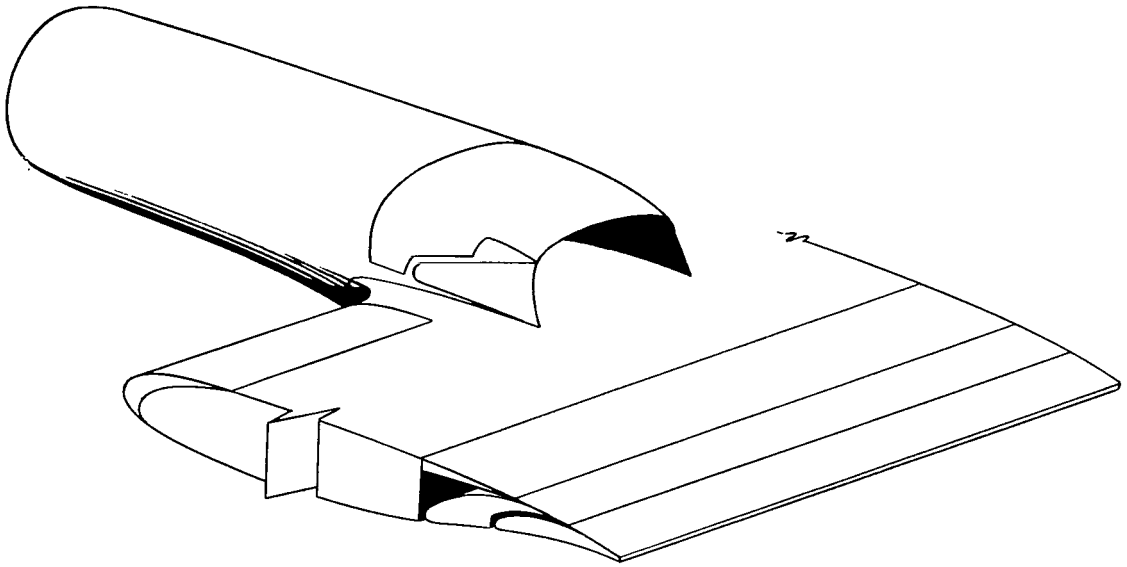

(a) Cruise configuration.

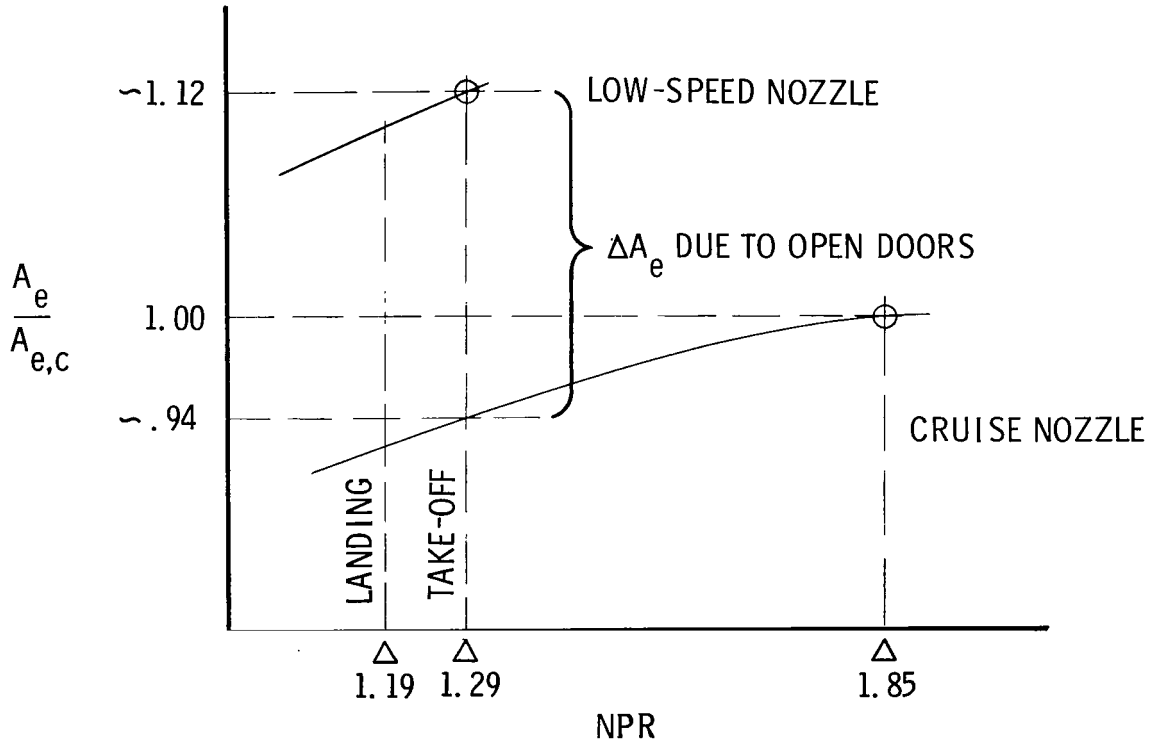

(b) Exit-area variation required for QCSEE USB engine.

Figure 2.- QCSEE USB nacelle concept.

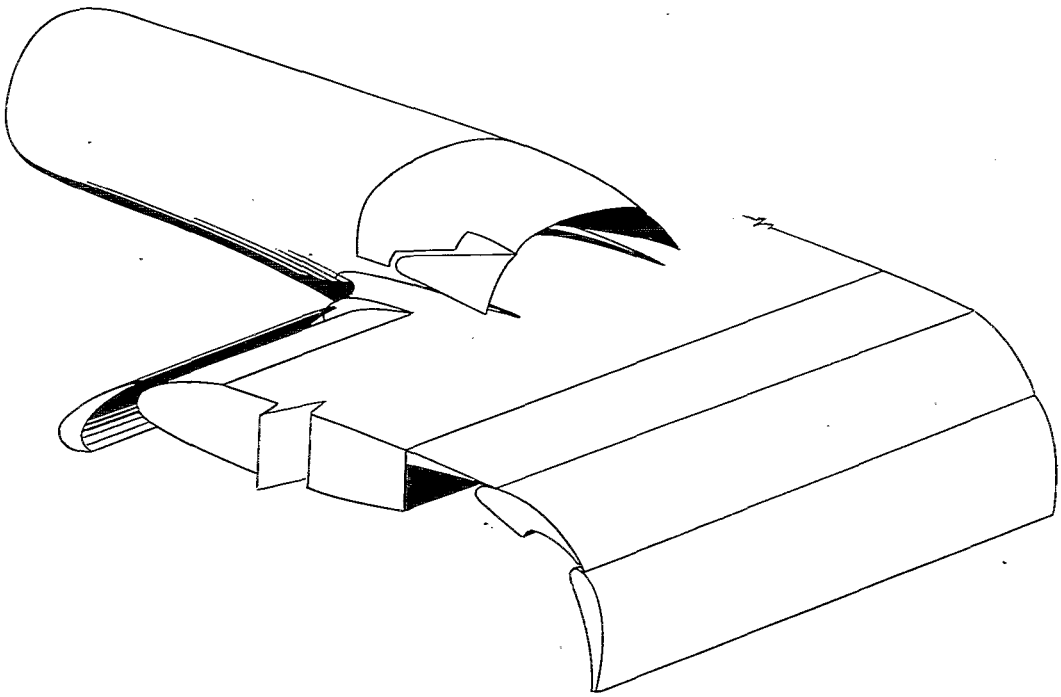

(c) Low-speed configuration shown with landing flap deflection.

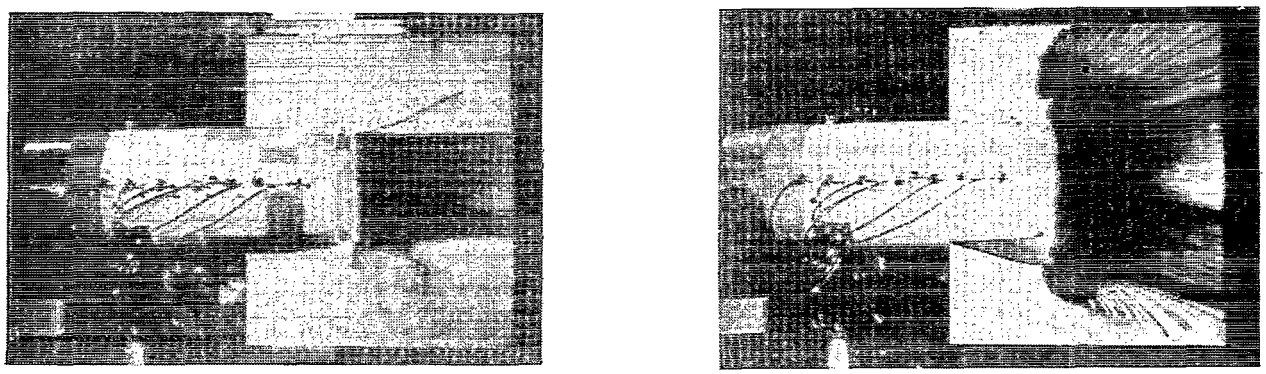

CRUISE CONFIGURATION - DOORS CLOSED

LOW-SPEED CONFIGURATION - DOORS OPEN

L-77-192

(d) Effect of open side doors on flow spreading. NPR = 1.2.

Figure 2.- Concluded.

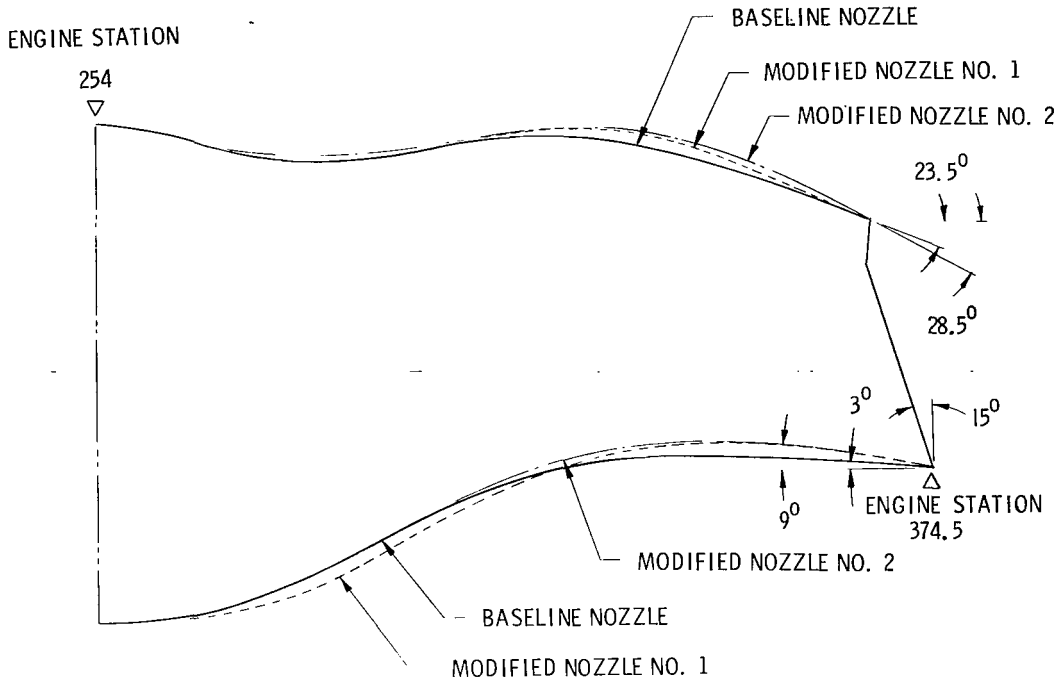

Figure 3.- QCSEE D-nozzle modifications.

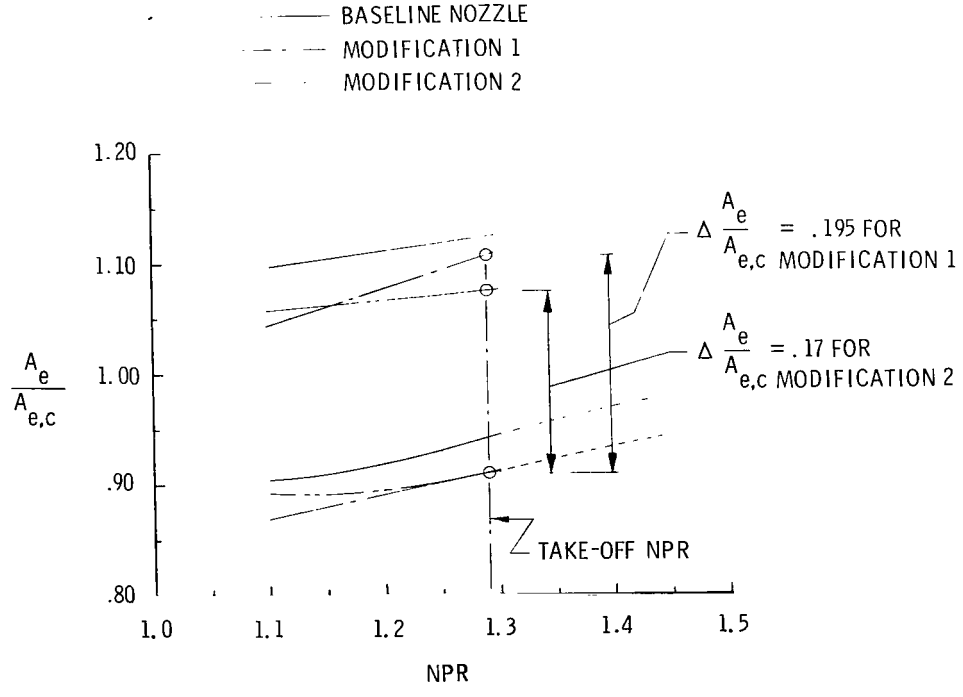

Figure 4.- Variation of effective exit area, compared with cruise exit area, for three D-nozzles.

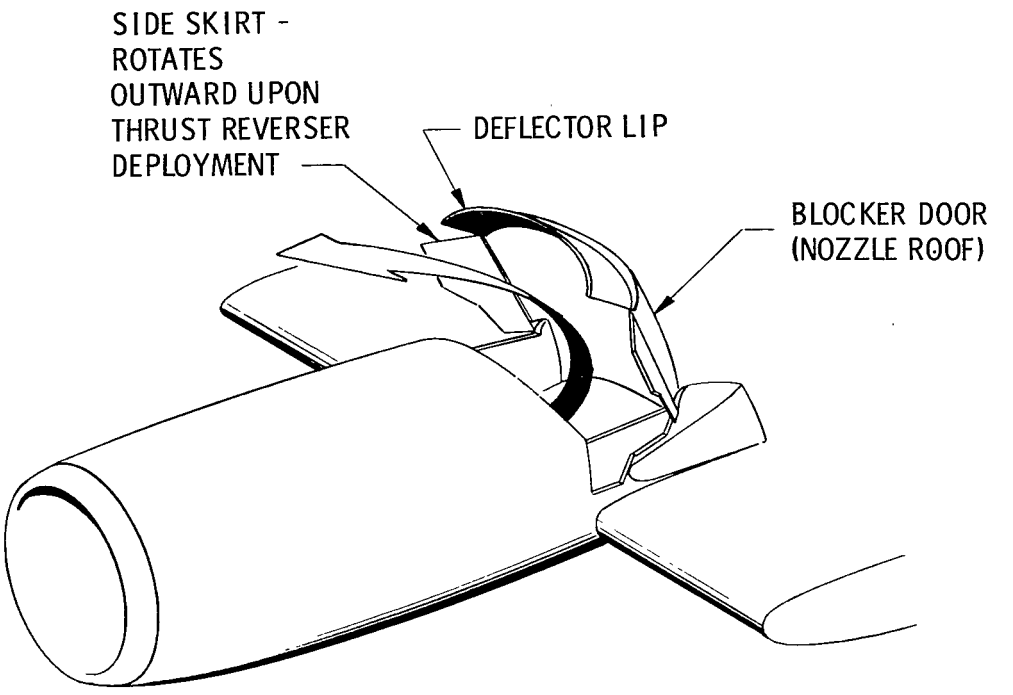

(a) Sketch of single-target thrust-reverser concept.

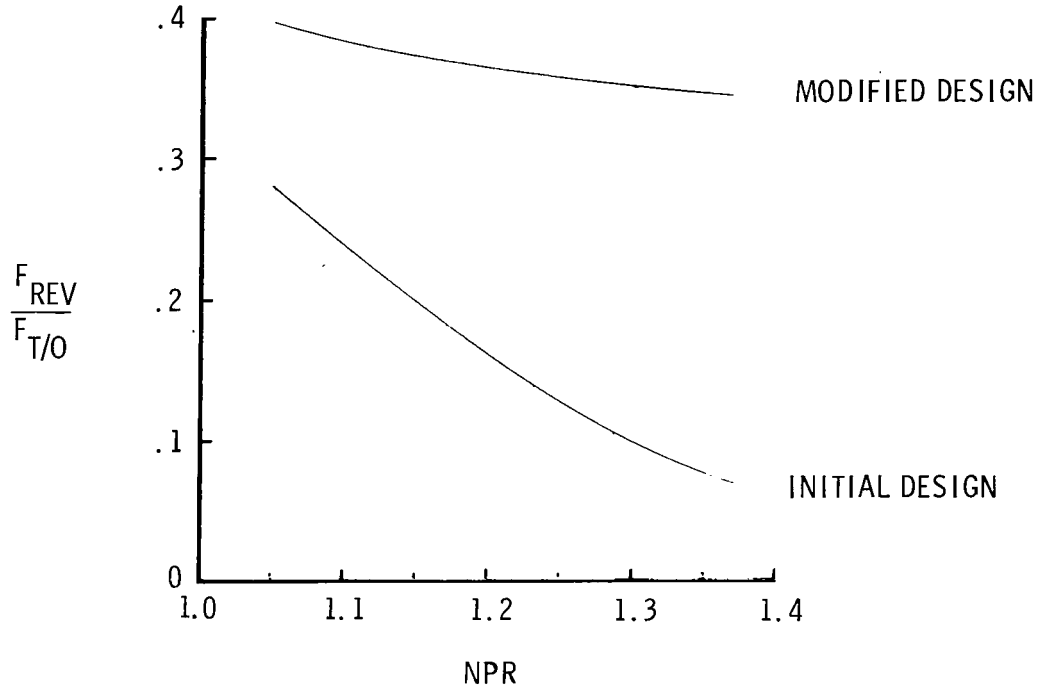

(b) Summary of reverse-thrust performance for initial and modified thrust-reverser designs.

Figure 5.- Thrust reverser for QCSEE D-nozzle.

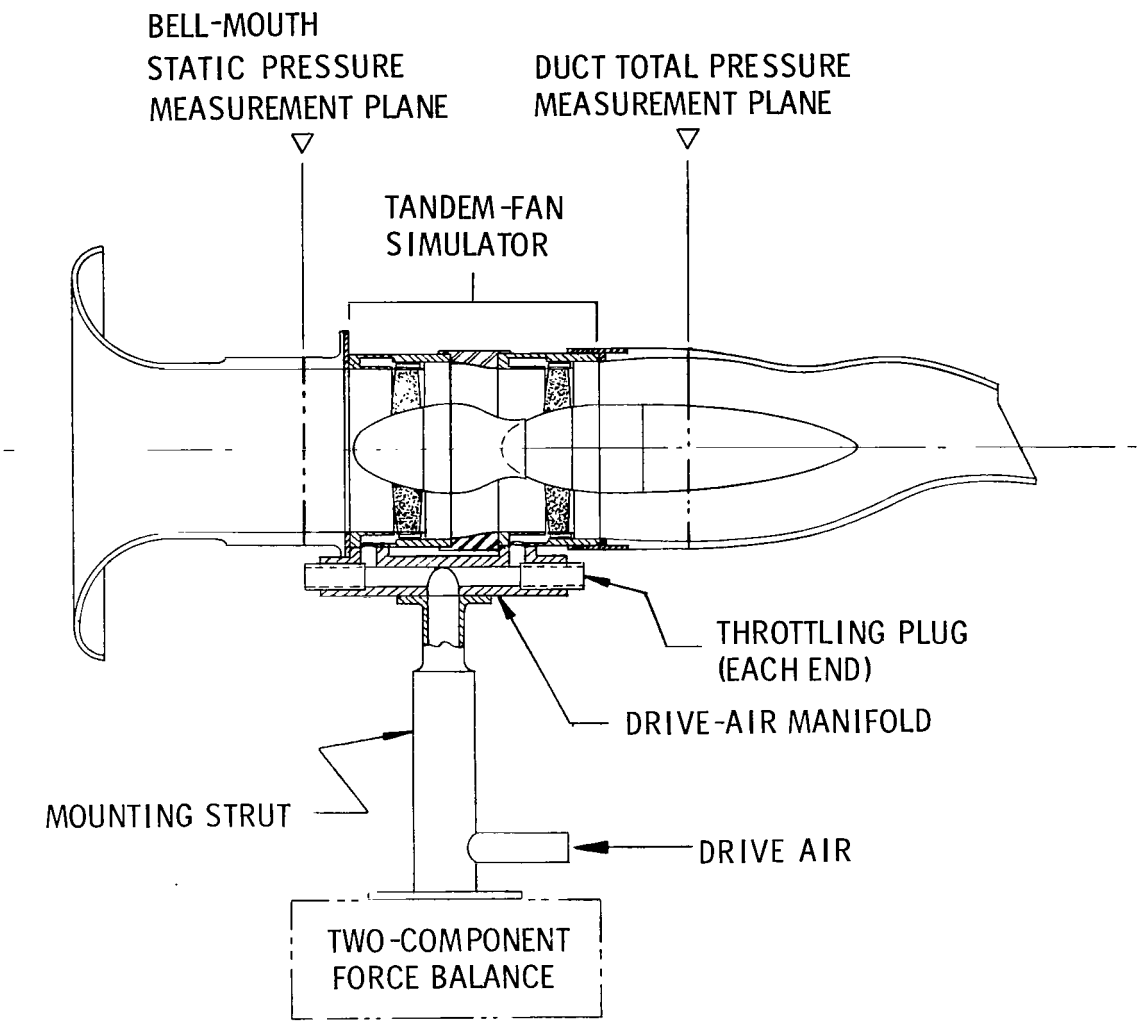

(a) Tandem-fan simulator and D-nozzle assembly.

Figure 6.- Static test model.

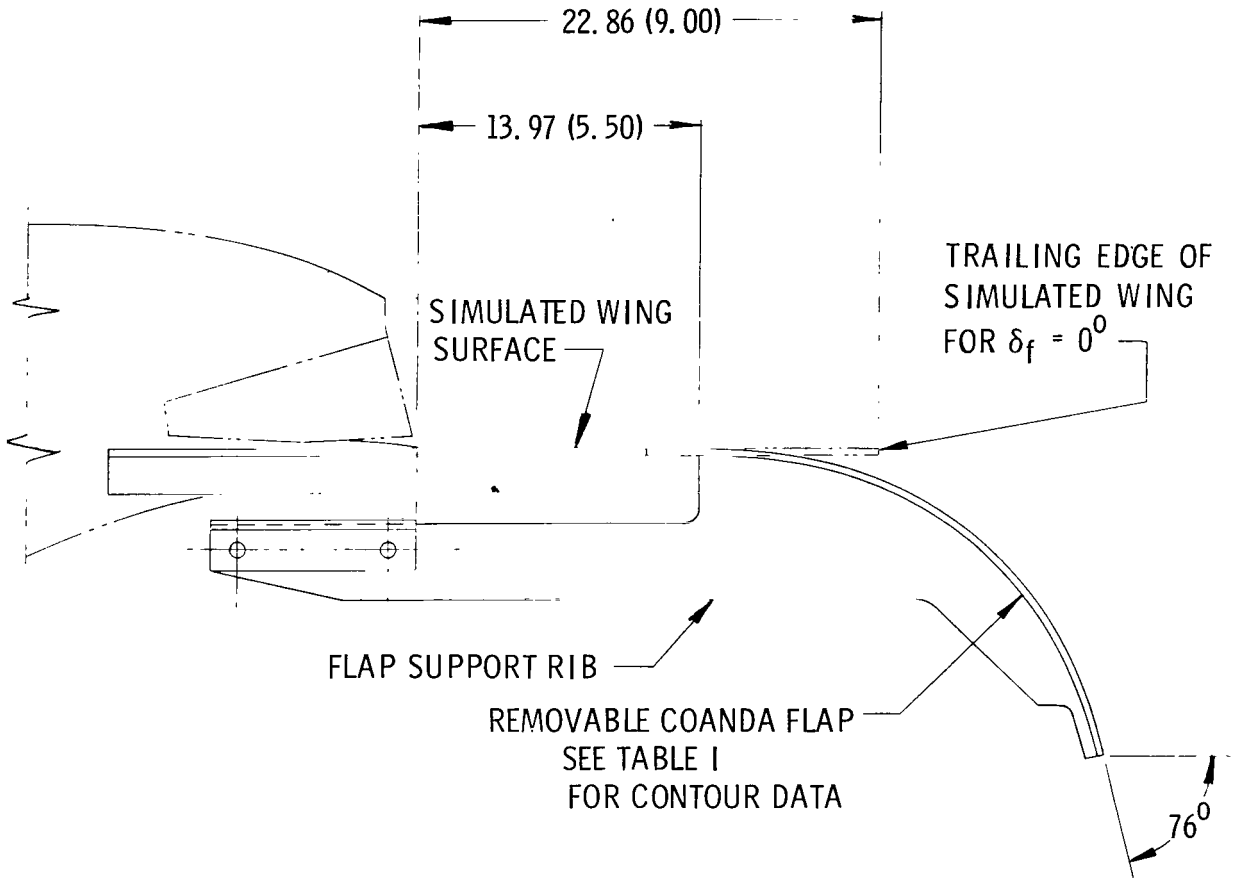

(b) Details of simulated wing and Coanda flap used on static model. Dimensions are in centimeters (inches).

Figure 6.- Continued.

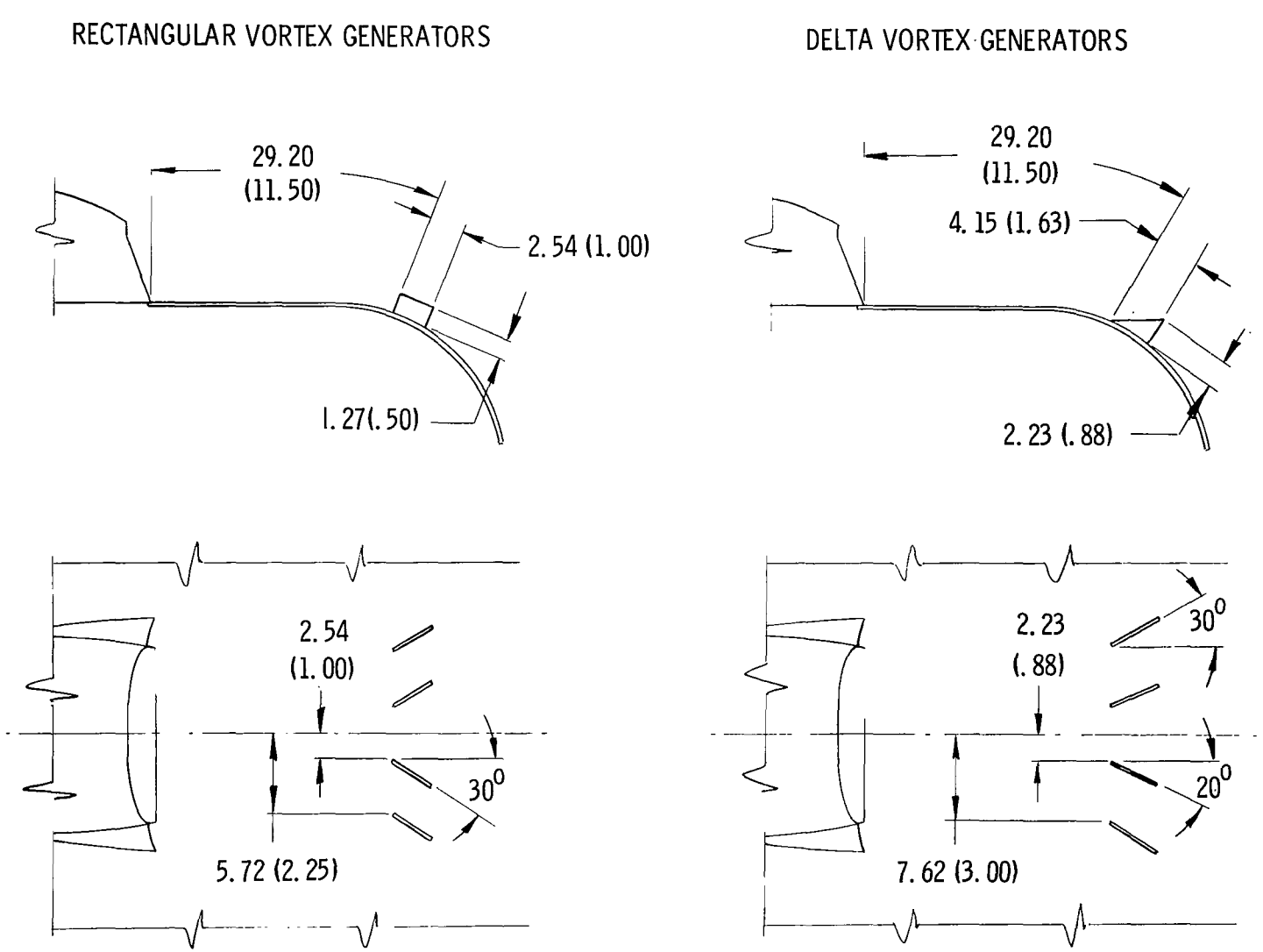

(c) Vortex generators. Dimensions are in centimeters (inches).

Figure 6.- Concluded.

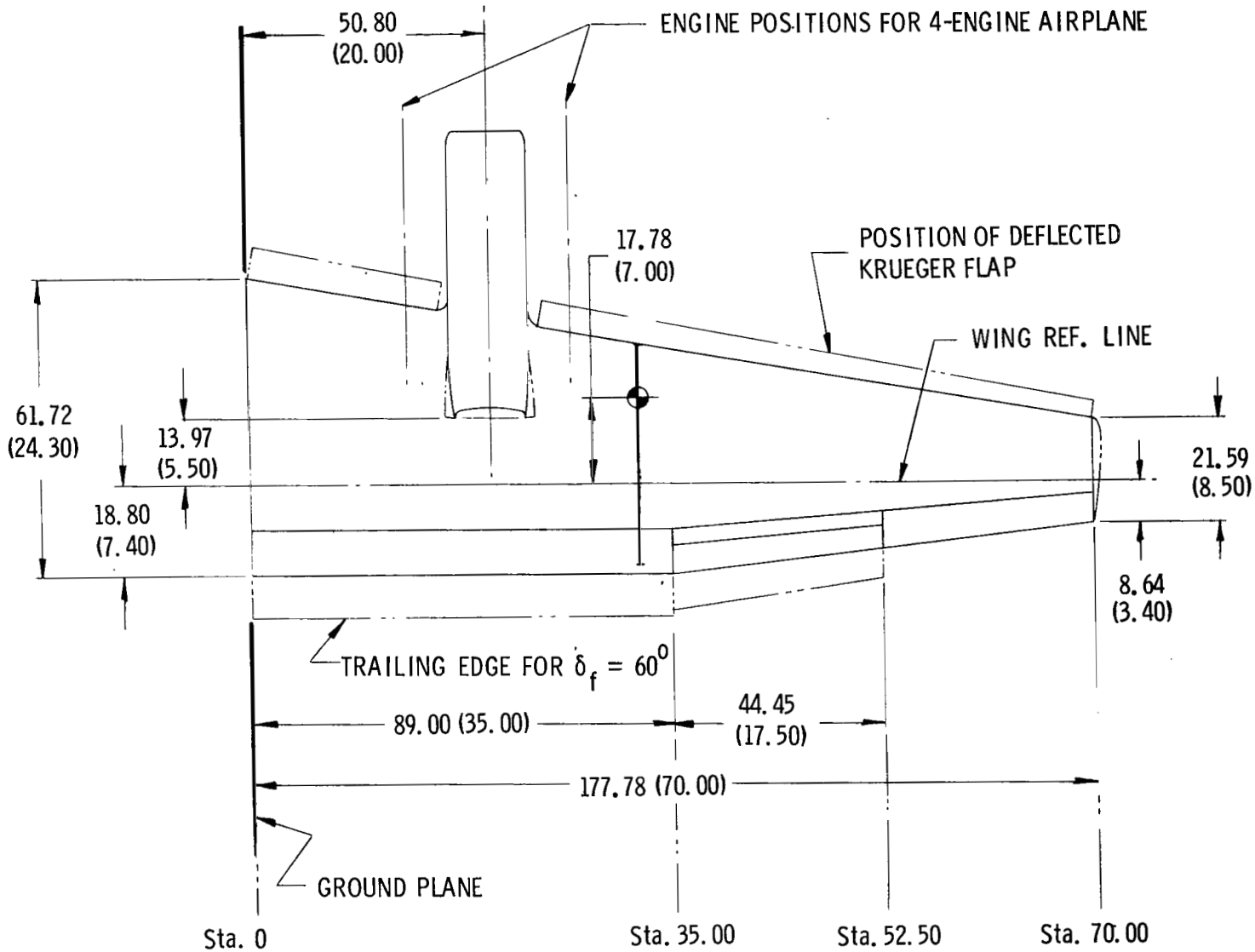

(a) General arrangement. Dimensions are in centimeters (inches).

Figure 7.- Semispan wing used in wind-tunnel tests.

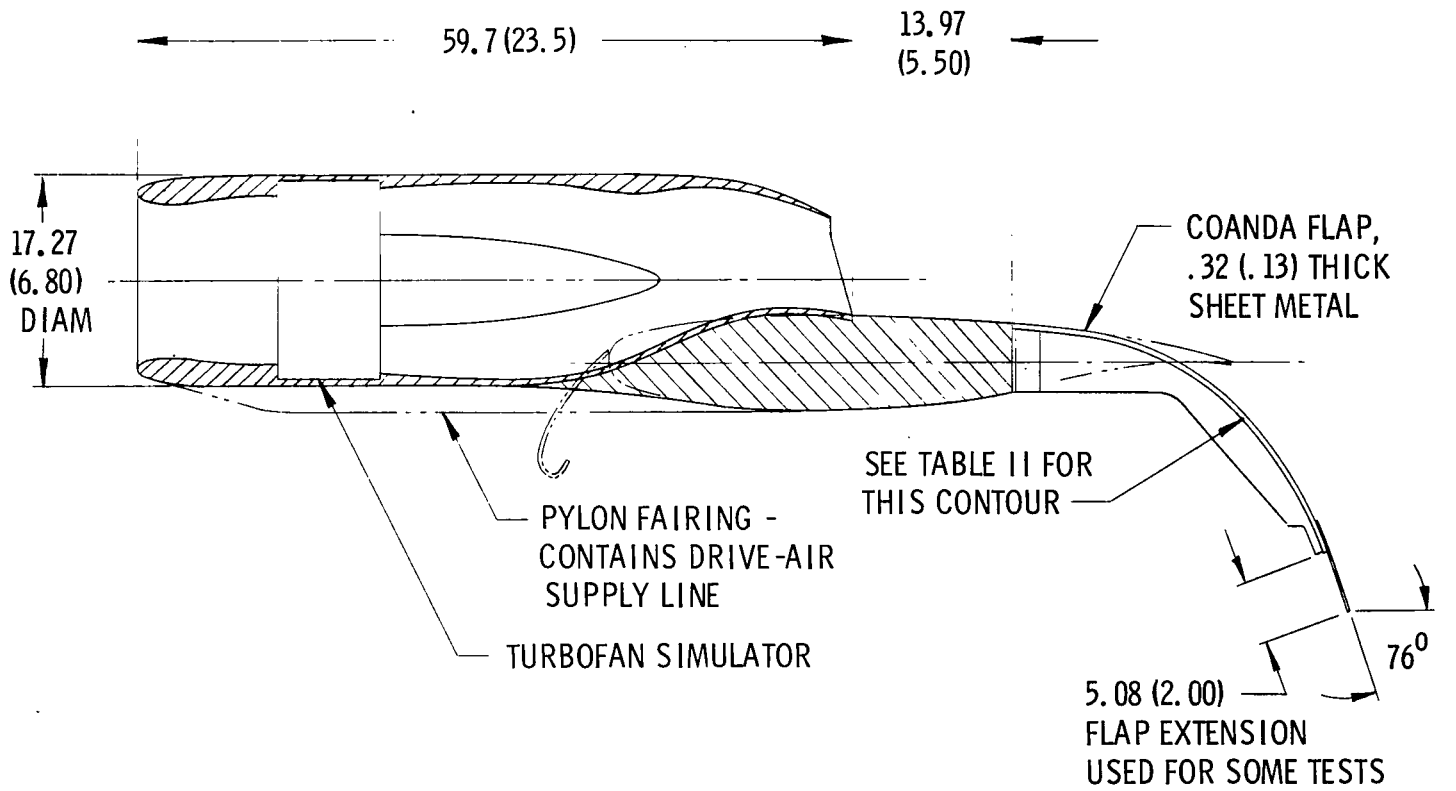

(b) Engine installation. Dimensions are in centimeters (inches).

Figure 7.- Continued.

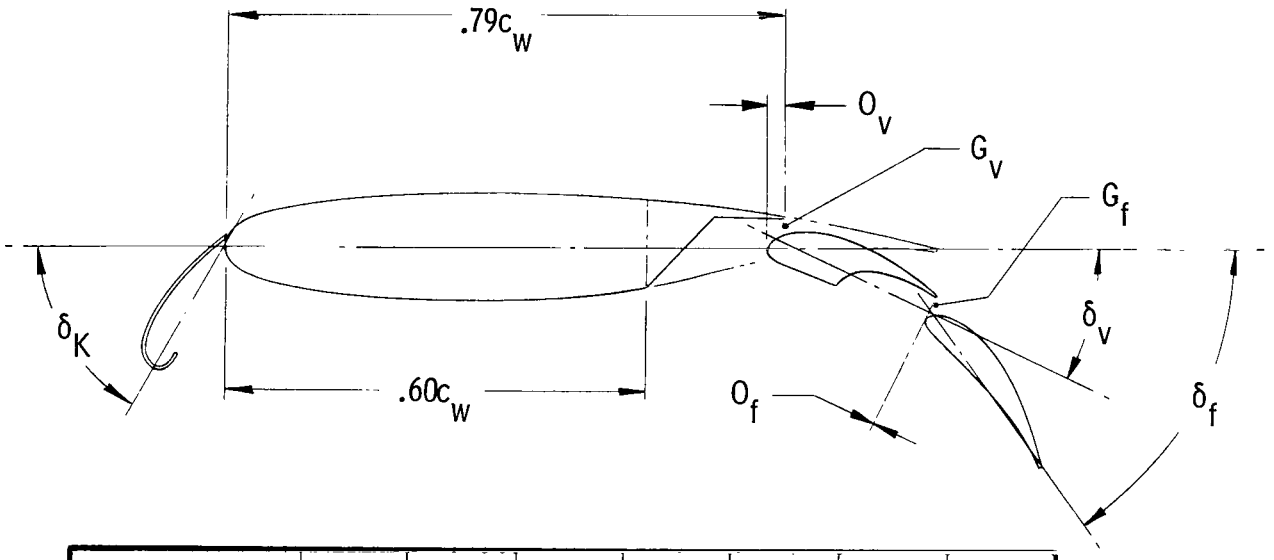

WING STA	δ_K	δ_v	O_v	G_v	δ_f	O_f	G_f
35.00	70^0	30^0	2.00	2.50	60^0	0	2.50
52.50	60^0	30^0	2.00	2.50	60^0	0	2.50
70.00	40^0	0	0	0	0	0	0

(c) Details of leading-edge Krueger flap and trailing-edge double-slotted flap. Dimensions are in percent c_w.

Figure 7.- Concluded.

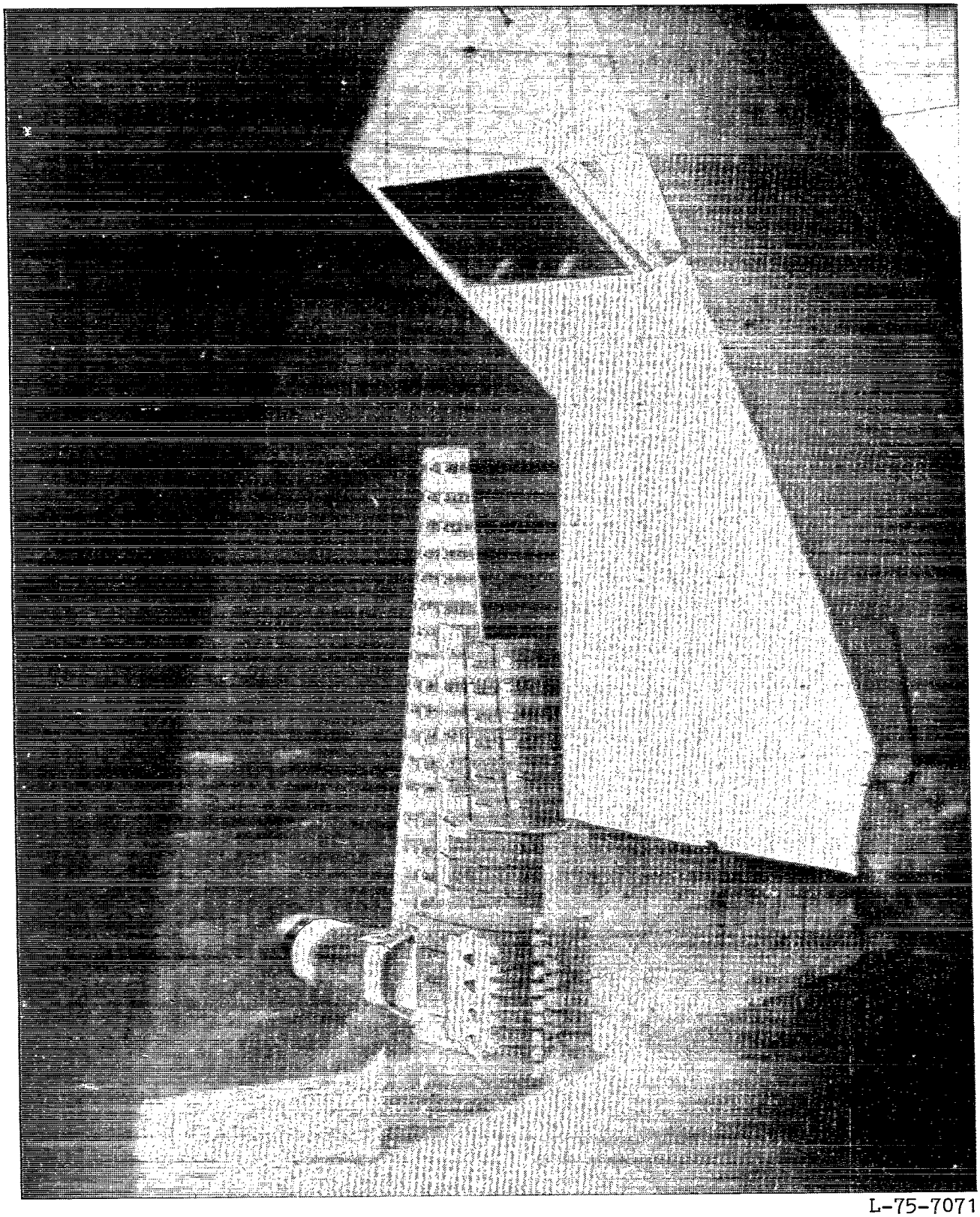

L-75-7071

Figure 8.- Photograph of wind-tunnel model mounted for force testing.

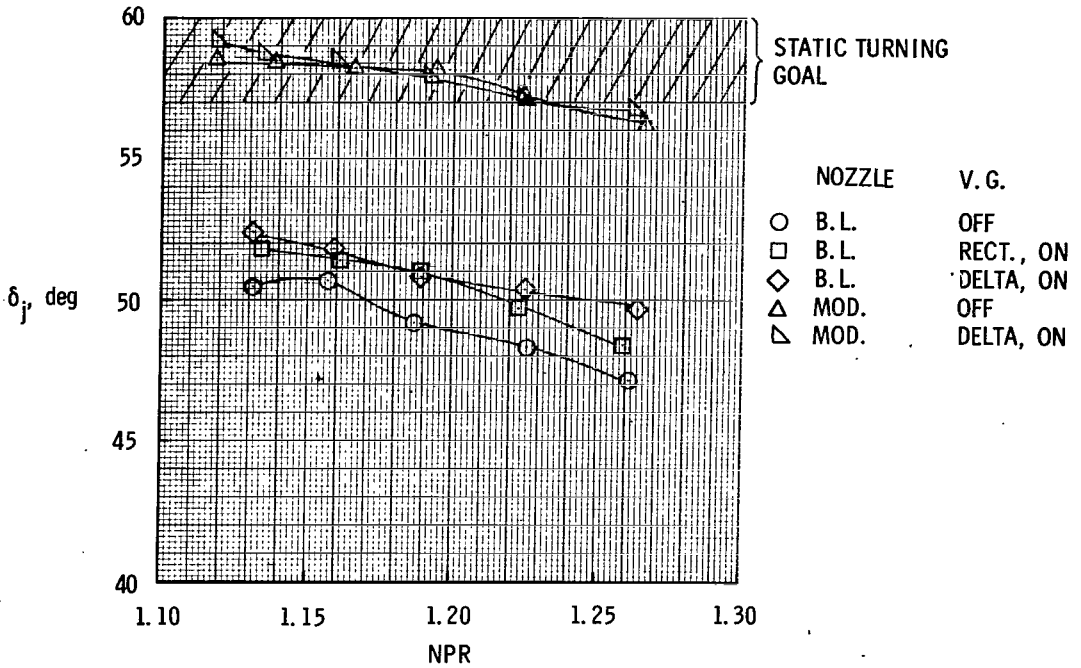

(a) Turning angle.

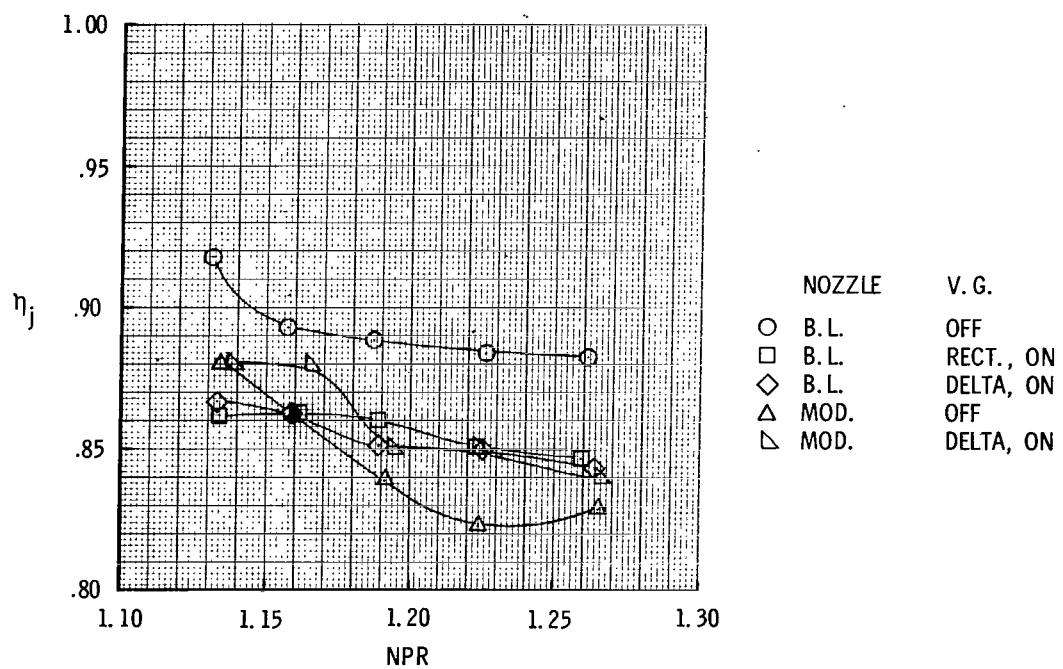

(b) Thrust-recovery efficiency.

Figure 9.- Static turning performance of low-speed nozzle. Side-door angle = 25°.

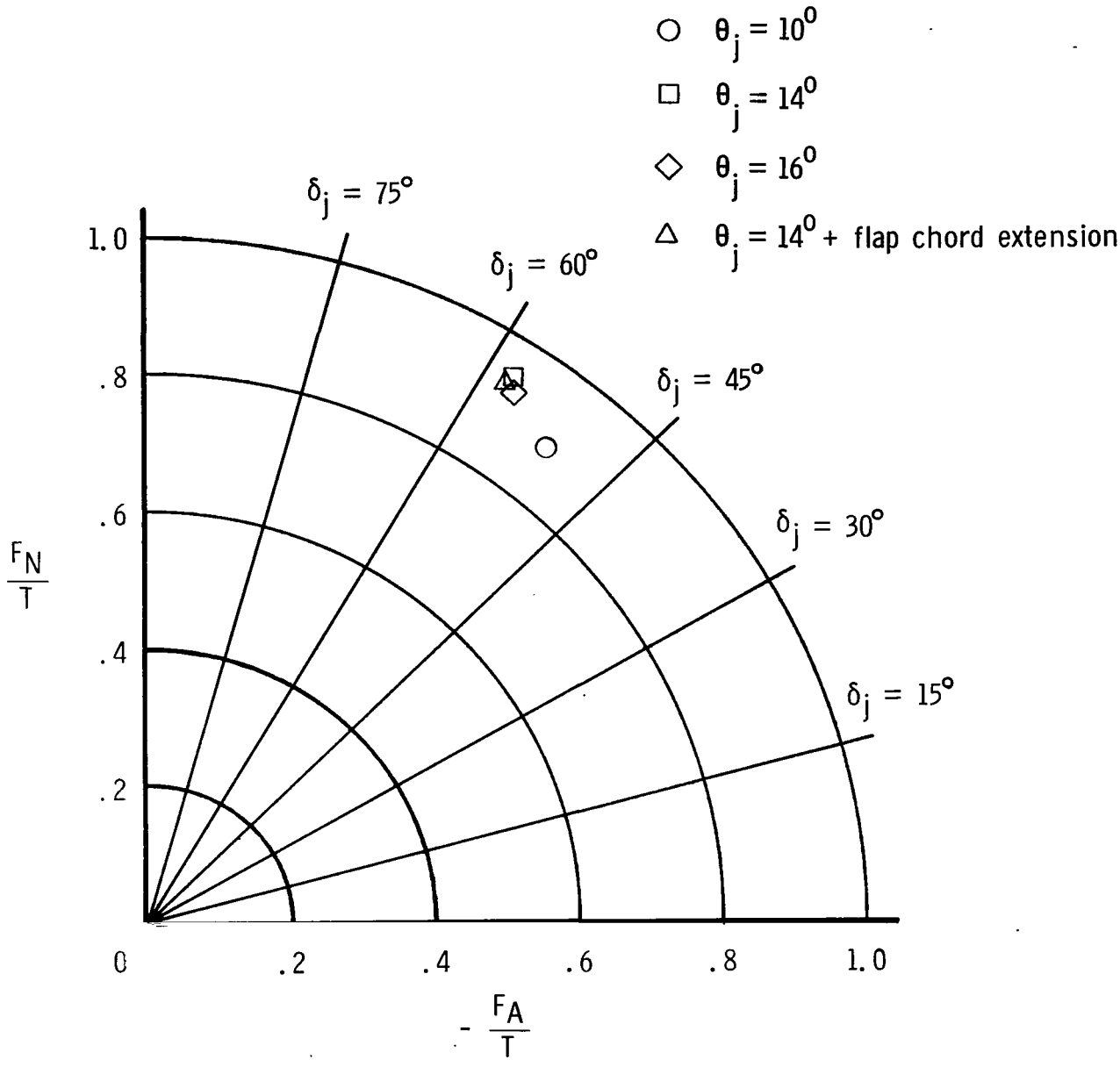

Figure 10.- Effect of kickdown angle on static turning performance of modified nozzle mounted on wind-tunnel wing-flap assembly. NPR = 1.2.

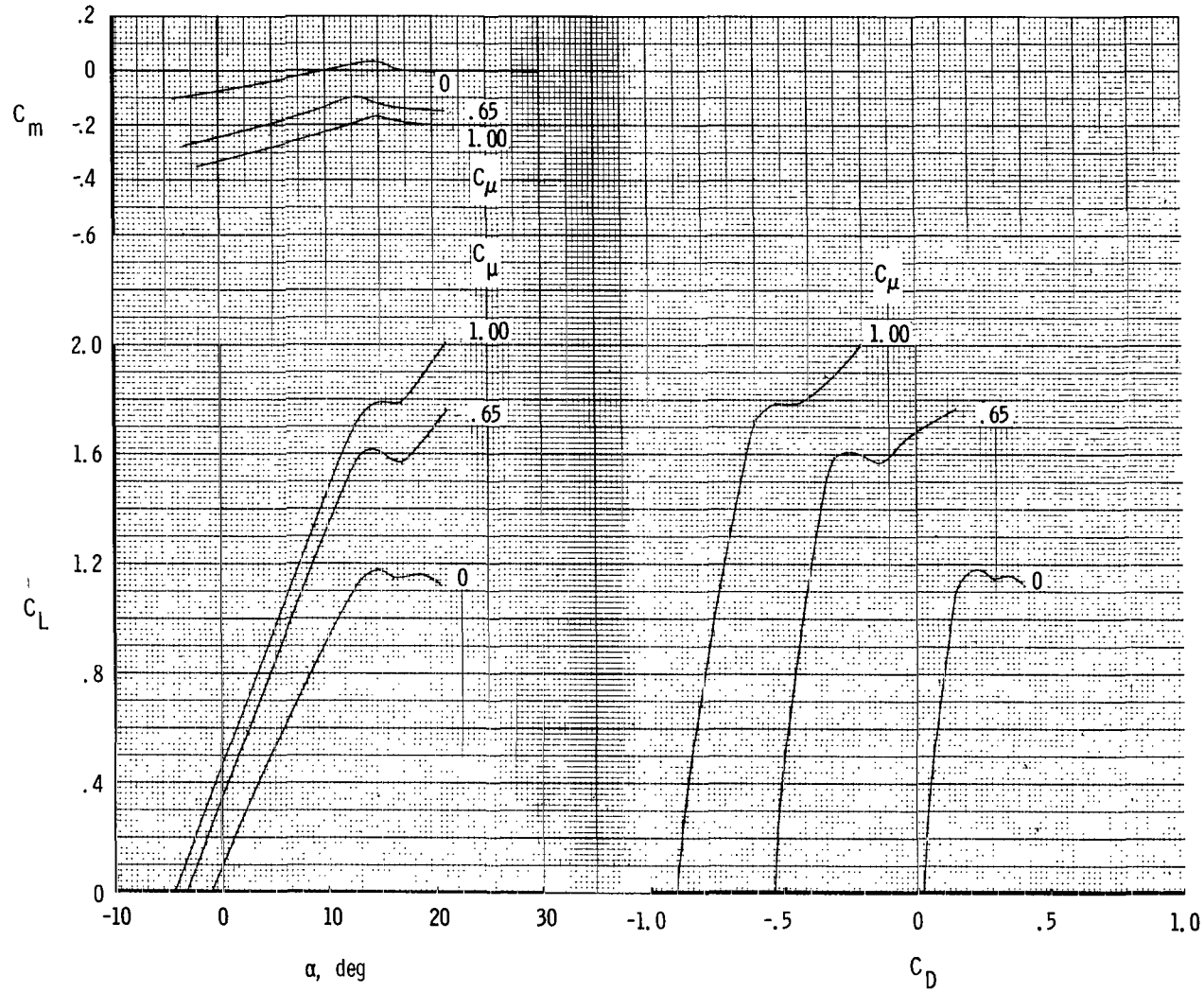

(a) $\delta_f = 0^o$; side doors closed.

Figure 11.- Longitudinal aerodynamic characteristics of model with baseline nozzle.

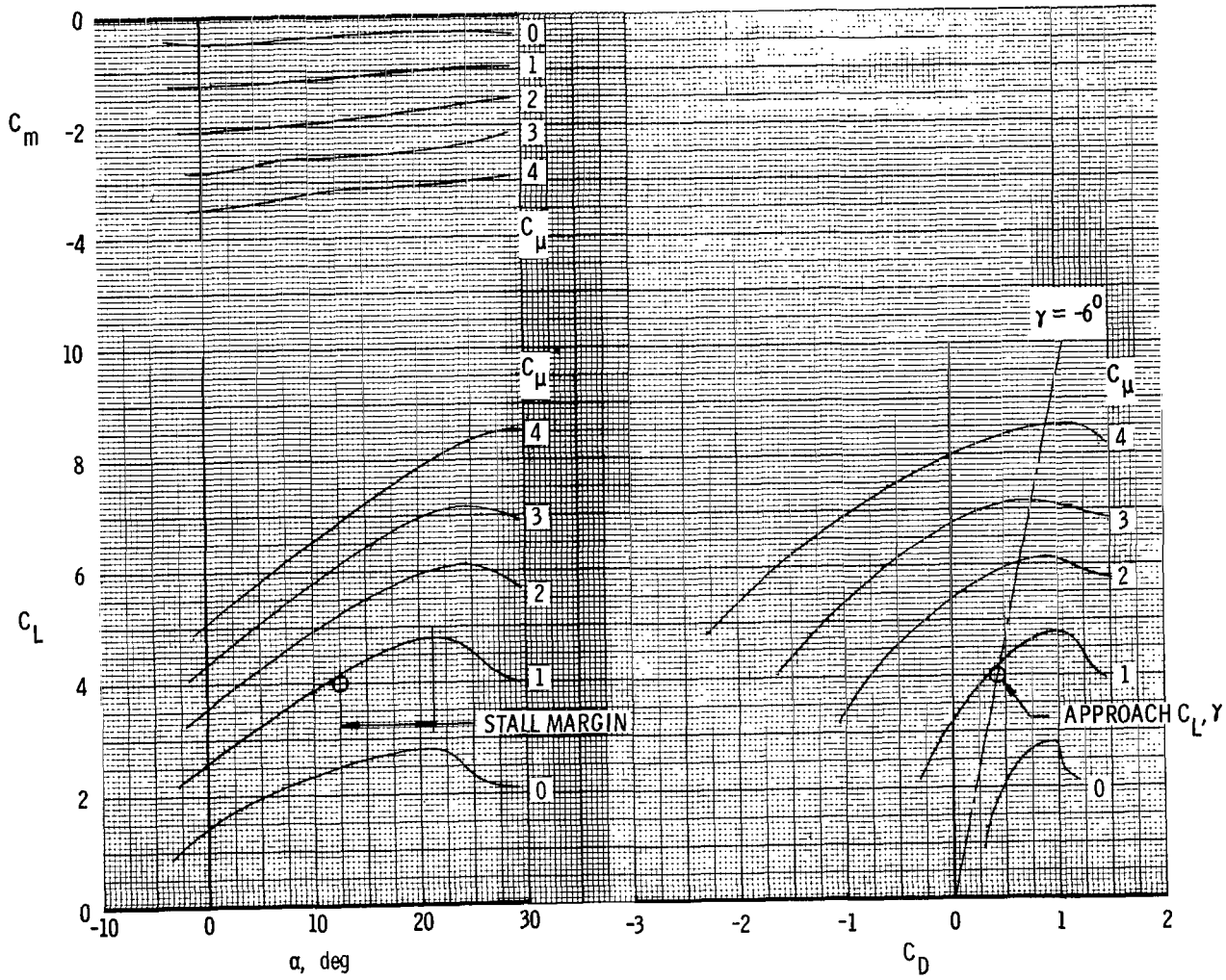

(b) $\delta_f = 60^o$; side-door angle = 25^o.

Figure 11.- Concluded.

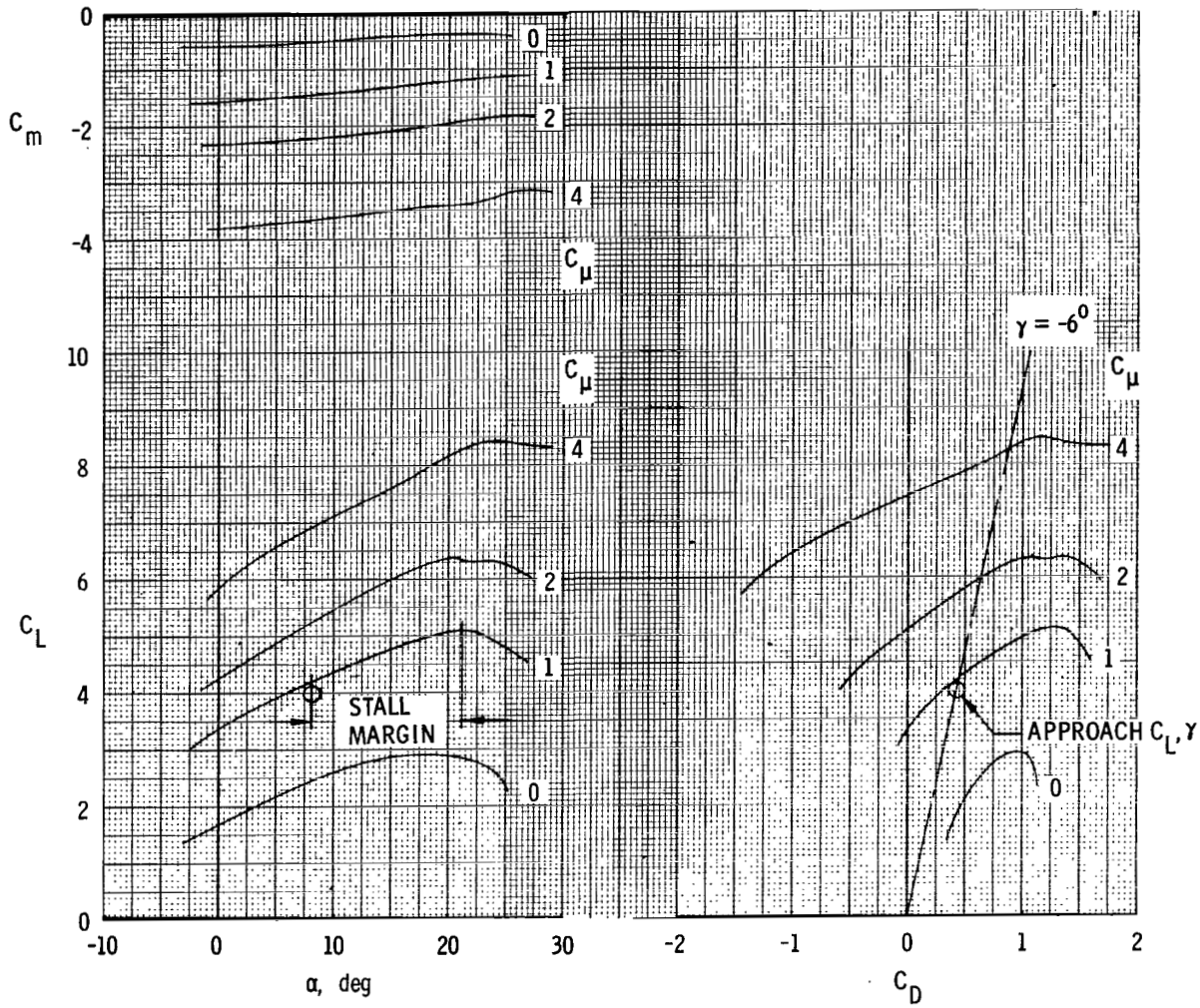

Figure 12.- Longitudinal aerodynamic characteristics of model with baseline nozzle and delta vortex generators. δ_f = 60°; side-door angle = 25°.

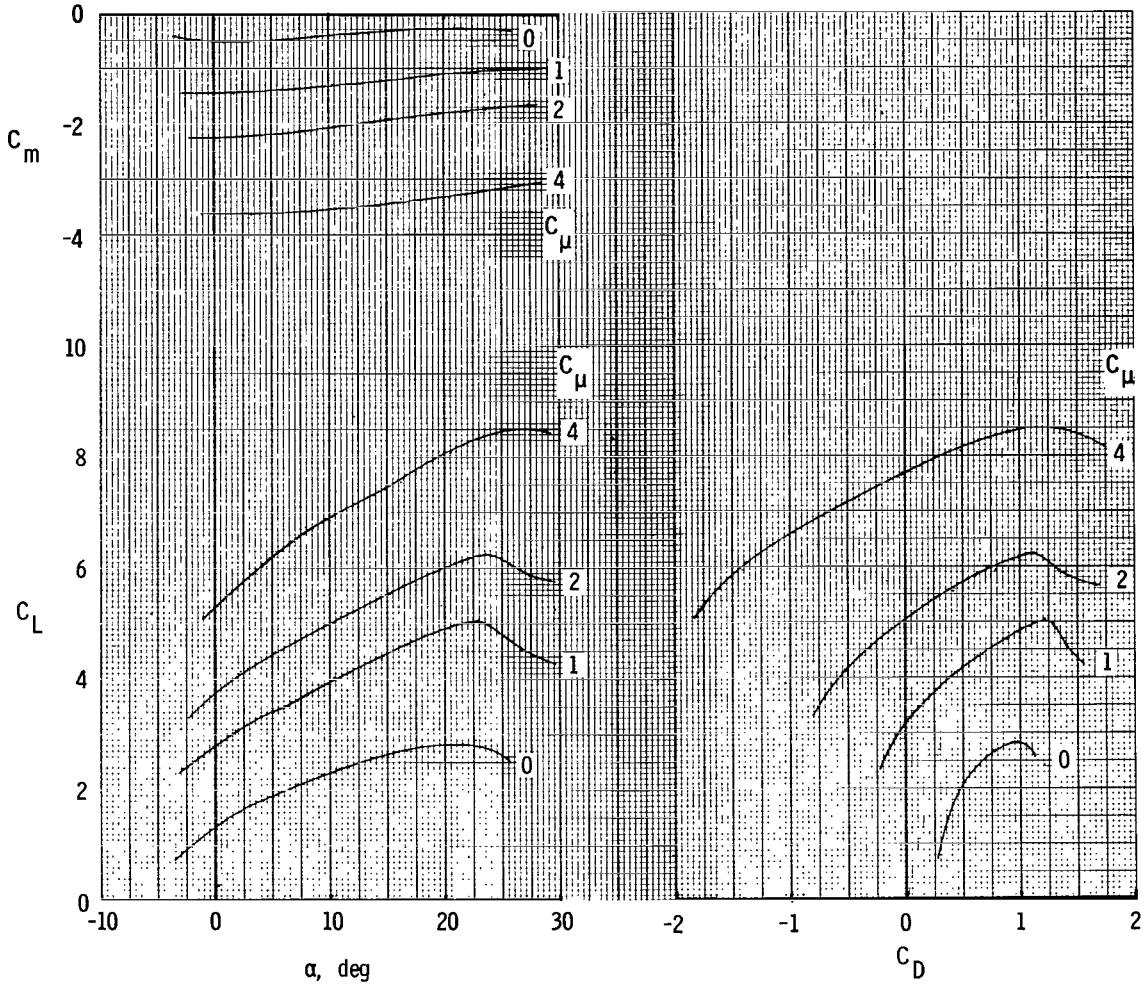

(a) $\theta_j = 10^o$.

Figure 13.- Longitudinal aerodynamic characteristics of model with modified nozzle. $\delta_f = 60^o$; side-door angle = 25^o.

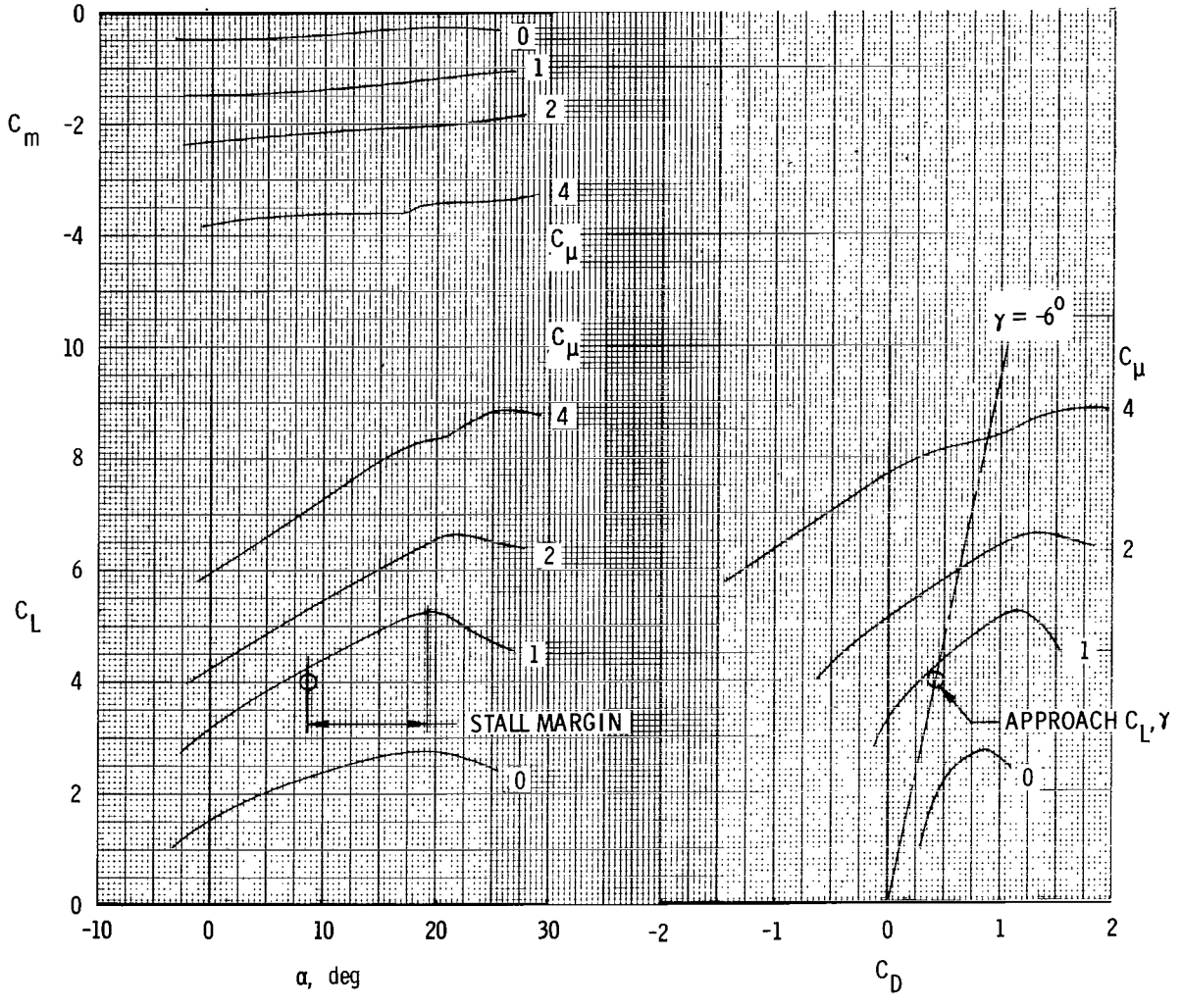

(b) $\theta_j = 14^o$.

Figure 13.- Continued.

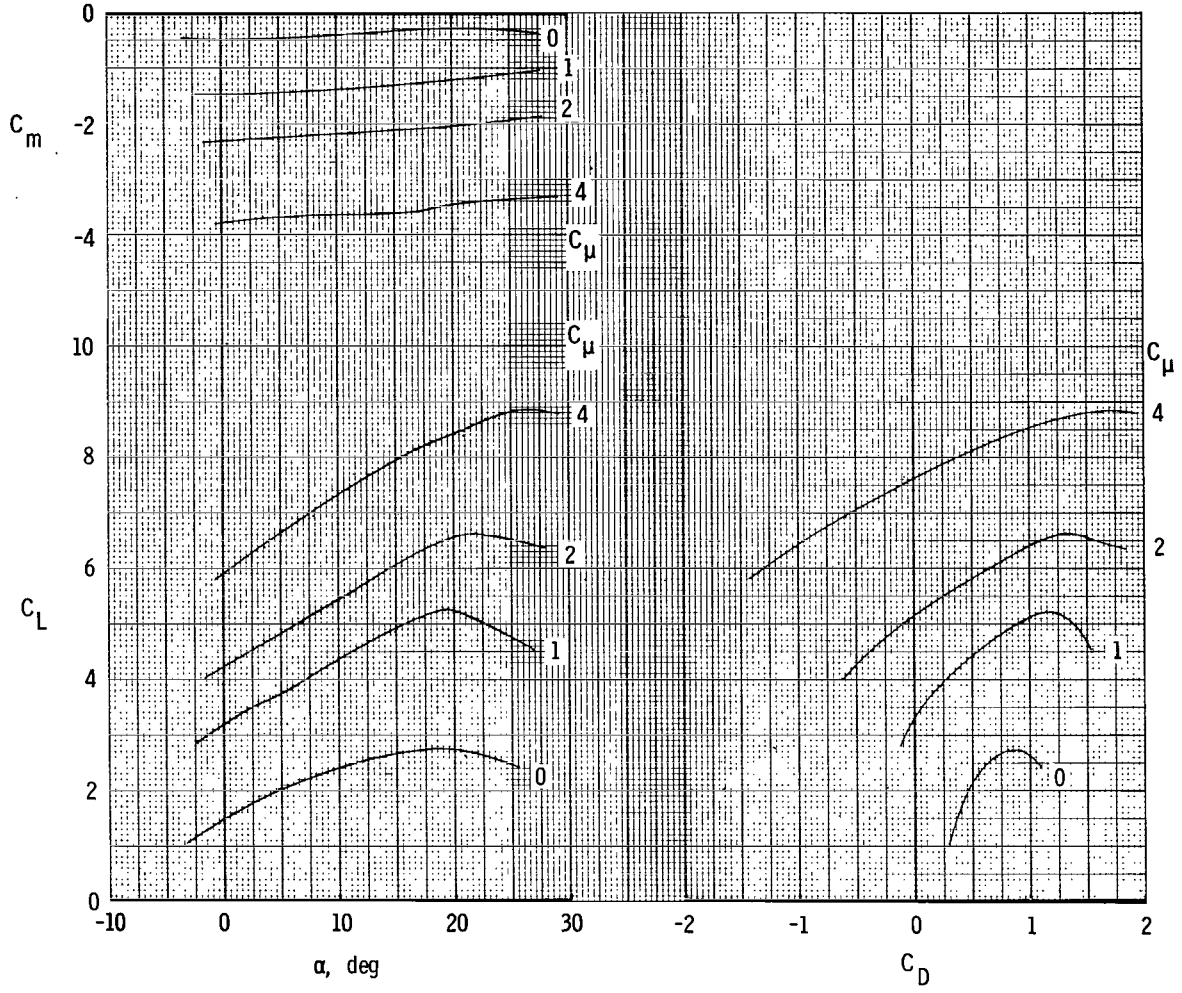

(c) θ_j = 16°.

Figure 13.- Concluded.

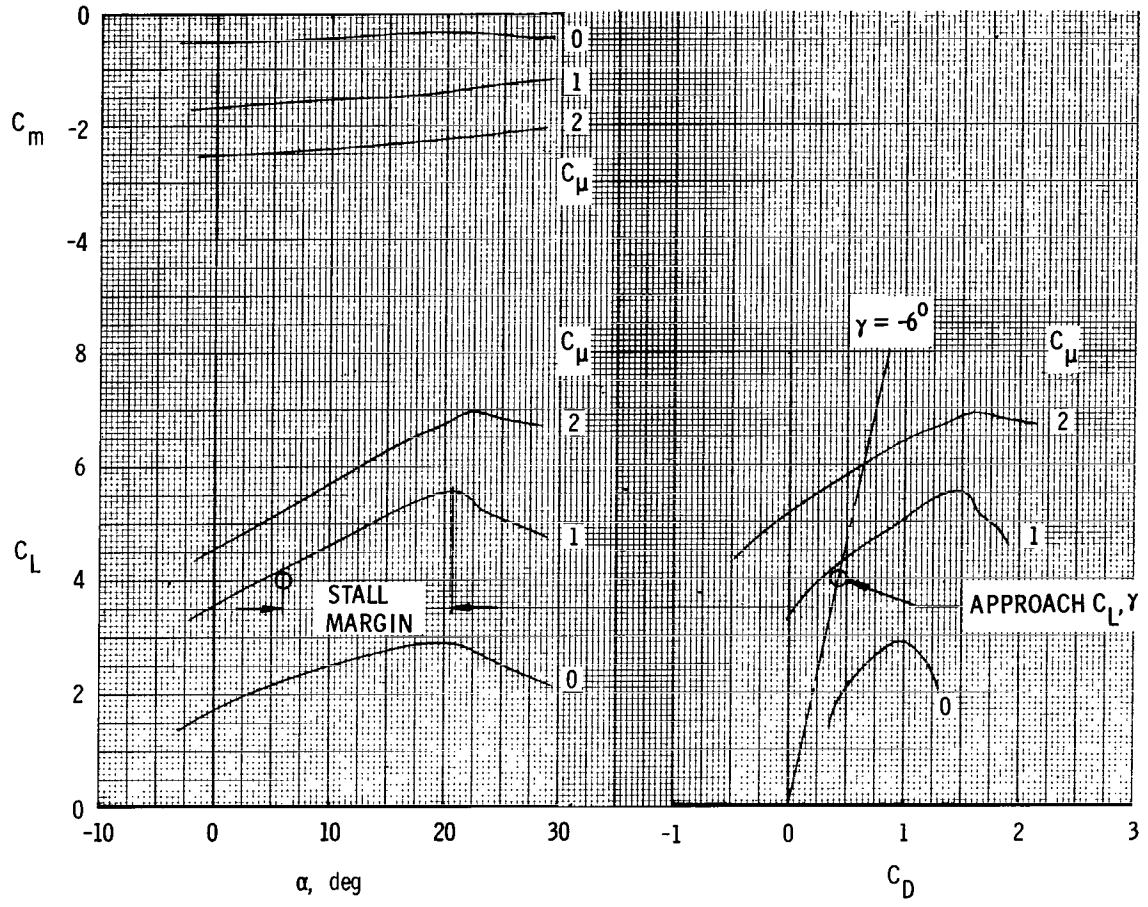

Figure 14.- Longitudinal aerodynamic characteristics of model with modified nozzle and flap chord extension. δ_f = 60°; side-door angle = 25°; θ_j = 14°.

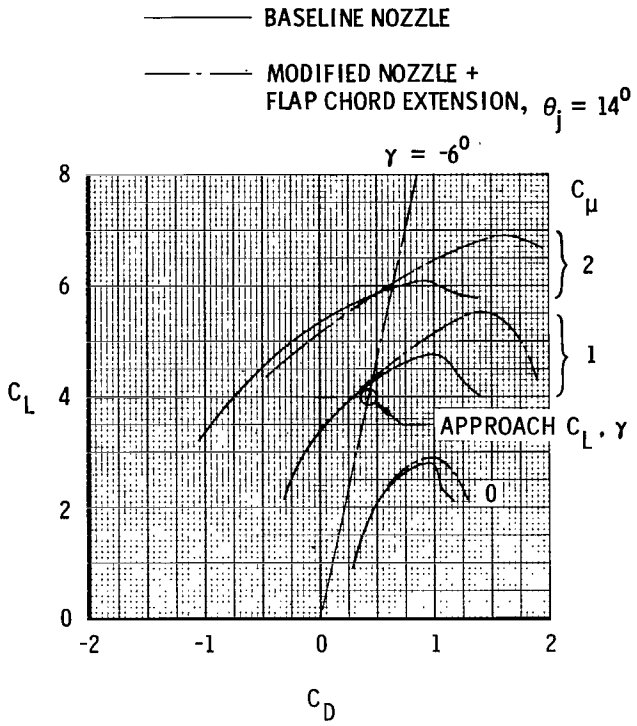

Figure 15.- Drag polars of baseline and modified configurations. $\delta_f = 60^o$.

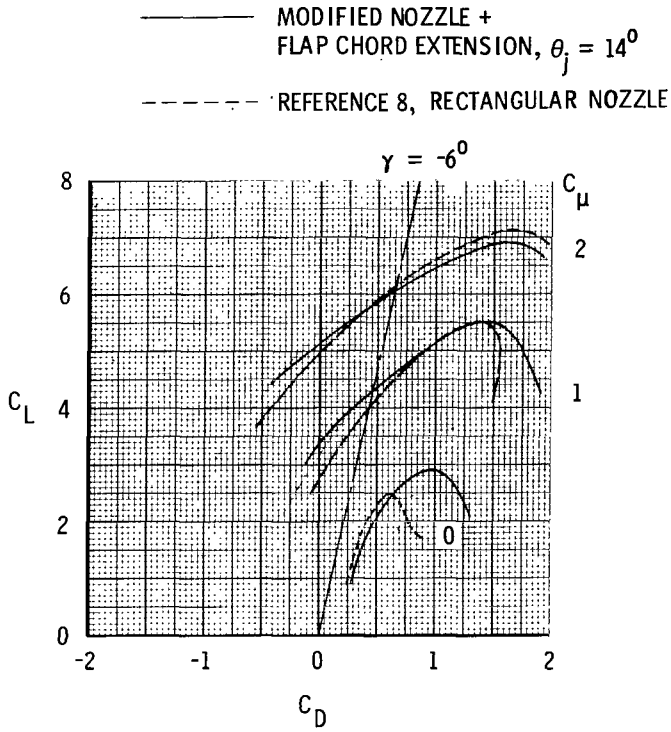

Figure 16.- Comparison of drag polars of configurations having rectangular and D-shaped nozzles. $\delta_j = 57^\circ$.

"The aeronautical and space activities of the United States shall be conducted so as to contribute . . . to the expansion of human knowledge of phenomena in the atmosphere and space. The Administration shall provide for the widest practicable and appropriate dissemination of information concerning its activities and the results thereof."

—NATIONAL AERONAUTICS AND SPACE ACT OF 1958

NASA SCIENTIFIC AND TECHNICAL PUBLICATIONS

TECHNICAL REPORTS: Scientific and technical information considered important, complete, and a lasting contribution to existing knowledge.

TECHNICAL NOTES: Information less broad in scope but nevertheless of importance as a contribution to existing knowledge.

TECHNICAL MEMORANDUMS: Information receiving limited distribution because of preliminary data, security classification, or other reasons. Also includes conference proceedings with either limited or unlimited distribution.

CONTRACTOR REPORTS: Scientific and technical information generated under a NASA contract or grant and considered an important contribution to existing knowledge.

TECHNICAL TRANSLATIONS: Information published in a foreign language considered to merit NASA distribution in English.

SPECIAL PUBLICATIONS: Information derived from or of value to NASA activities. Publications include final reports of major projects, monographs, data compilations, handbooks, sourcebooks, and special bibliographies.

TECHNOLOGY UTILIZATION PUBLICATIONS: Information on technology used by NASA that may be of particular interest in commercial and other non-aerospace applications. Publications include Tech Briefs, Technology Utilization Reports and Technology Surveys.

Details on the availability of these publications may be obtained from:

SCIENTIFIC AND TECHNICAL INFORMATION OFFICE

NATIONAL AERONAUTICS AND SPACE ADMINISTRATION

Washington, D.C. 20546